# A sequential minimisation algorithm based on the convexification approach

**Michael V. Klibanov† and Alexandre Timonov†**

† Department of Mathematics, University of North Carolina at Charlotte, Charlotte, NC 28223, USA

E-mail: mklibanv@email.uncc.edu, atimonov@email.uncc.edu

**Abstract.**

A sequential minimisation algorithm for the numerical solution of inverse problems of frequency sounding is presented. This algorithm is based on the concept of convexification of a multiextremal objective function proposed recently by the authors. A key point in the sequential minimisation algorithm is that unlike conventional layer-stripping algorithms, it provides the stable approximate solution via minimisation of a finite sequence of strictly convex objective functions resulted from applying the nonlinear weighted least squares method with Carleman's weight functions. Another advantage of the proposed algorithm is that the starting vectors for the descent methods of minimisation are directly determined from the data eliminating the uncertainty inherent to the local methods, such as the gradient or Newton-like methods. The 1-D inverse model of frequency sounding is selected to demonstrate its computational feasibility. Based on the localising property of Carleman's weight functions, it is proven that the distance between the approximate and "exact" solutions is small if the approximation error is small. The computational experiments with several realistic and synthetic marine shallow water configurations are presented to demonstrate the computational feasibility of the proposed algorithm.

## 1. Introduction

In a recent paper [1] the authors have presented a new approach to inverse problems of frequency sounding called the convexification. The essence of convexification is constructing the strictly convex objective functions when applying the least squares method to the nonlinear coefficient inverse problems. It has been demonstrated in [1] that the conventional residual objective functions may often be multiextremal. Under such a condition, the gradient and Newton-like methods do not guarantee the convergence to a global minimum. Therefore, the numerical methods of global optimisation, such as simulated annealing or genetic algorithms, are usually used to search for a global minimum. However, these methods are time-consuming even for several unknowns, and their use for solving the coefficient inverse problems has not been rigorously justified. The convexification approach can be considered as an alternative to the methods of global optimisation.

In principle, the convexification approach is applicable to many inverse problems of frequency sounding of inhomogeneous media. In this paper we focus on the inverse problem of magnetotelluric (MT) sounding of layered marine shallow water configurations (see Figure 1) and address rigorously the issue of multiextremality. Also, we demonstrate that the convexification approach can be applied to constructing a stable computational algorithm.

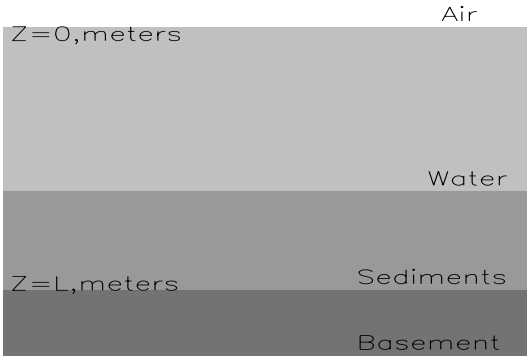


**Figure 1.** A typical marine shallow water configuration.

The main advantage of the convexification approach is that it does not require knowledge of the so-called background coefficient close to the "exact" solution. This is mainly because of the strict convexity of resulting objective functions. Briefly, the convexification approach consists of the following stages. The original coefficient inverse problem is identically transformed to a certain auxiliary overdetermined boundary value problem for the nonlinear integro-differential equation that does not explicitly contain an unknown coefficient. The latter problem may also be interpreted in terms of continuation of the transformed field from the surface in an inhomogeneous layer. In the geophysics

literature, such a procedure is referred to as the field prediction. The integro-differential operator is approximated by a family of parametric operators, where the parameter is chosen to be an upper bound of the frequency band. After that, the nonlinear weighted least squares method is applied to reduce the problem of field prediction to a constrained minimisation problem. Once the transformed field in the inhomogeneous layer is found, the coefficient distribution is directly determined from this field. It should be emphasised that the use of Carleman's weight functions (CWF) is crucial for constructing the strictly convex objective functions.

Our specific choice of the model problem is motivated by the following. The principle of MT sounding was first formulated and investigated by Tikhonov [2, 3] and Cagniard [4] in the early fifties of the 20th century. Since then, the 1-D model of MT sounding has been extensively tested against a variety of simulated and field data for tectonic studies and geophysical exploration of mineral, oil and gas deposits (see, e.g., [5]). As a result, the consistency of this model with realistic horizontally-stratified (layered) media was well established. Over the last two decades, the MT sounding methods have also been applied to marine induction studies in oceanography (see, e.g., [6], [7]). Since the marine configurations consist of the highly conductive seawater and porous sediments, the wave process is not practically established in such media. Therefore, the propagation of the electromagnetic (EM) field at low frequencies is similar to the diffusion of light in highly absorbing media. It has been pointed out in the contemporary marine electromagnetics literature (see, e.g., [8]) that in shallow waters the EM signals can be accurately detected in the 1 Hz to 10 KHz frequency band. This frequency band is of particular interest to the Navy for underwater communication and navigation and detection and identification of objects submerged in the seawater or buried in the near-seafloor sediments. Actually, these applications require the use of controlled EM sources, such as electric or magnetic dipoles or line currents, to provide higher frequencies of operation and larger transmitter currents of the order of $10^2$ ampers. However, it can be shown (see Appendix A) that in the case of electric or magnetic dipoles, the EM frequency sounding models with respect to components of the vector potential are similar to the MT model (see (2.6)-(2.8) in Section 2.1). Therefore, one can take advantage of exploiting the 1-D MT model in demonstrating the computational feasibility of the convexification approach.

The MT (EM) sounding observations are usually available in the limited frequency band $[\tilde{\omega}_{min}, \tilde{\omega}_{max}]$ due to both the physical and logistic reasons. In marine electromagnetics, the upper bound does not exceed few hundred Hz. In other words, the sounding data are always incomplete. Furthermore, the application of the Tikhonov regularisation scheme to a nonlinear inverse problem (see, e.g., [9], [10]) does not, in general, eliminate the multiextremality of Tikhonov's smoothing functional. Indeed, if the regularisation parameter $\alpha$ is sufficiently large, the stabilising term in Tikhonov's smoothing functional dominates over the residual one. Since the stabilising term is quadratic, Tikhonov's functional may become even quasi-strictly convex. However, the minimiser of this functional may be sufficiently far from the "exact" solution.

Conversely, if the regularisation parameter is sufficiently small, the residual term dominates over the stabilising one. So, the multiextremality of Tikhonov's smoothing functional may remain. It is clear that under this condition, the problem of choosing the proper regularisation parameter $\alpha$ is crucial.

Since the eighties of the 20th century, the $\alpha$-dependence of Tikhonov's smoothing functional has been extensively exploited in the Soviet (Russian) geophysics community (see, e.g., [11], [5]) when applying various gradient and Newton-like methods to inverse problems of MT (EM) frequency sounding. Specifically, starting with sufficiently large value of $\alpha$, the minimisation problem for Tikhonov's smoothing functional is solved by either the gradient or Newton-like methods. The process is advancing in the direction of decrease of $\alpha$ until a certain stopping criterion is attained. In [12] such a technique for choosing the regularisation parameter was formalised and referred to as the continuation method. In the contemporary mathematics literature (see, e.g., [9], [13]), this technique is referred to as outer-inner iterations (an outer iteration over $\alpha$ and an inner iteration with a gradient or Newton-like method). In [13], the outer-inner iteration scheme has been justified for one specific case when the original nonlinear operator can be decomposed into (or approximated by) a sum of linear and bilinear operators. However, the outer-inner iteration scheme require many restarting procedures if there is no *a priori* information available about a certain approximation to the "exact" solution located in its small vicinity. The convexification approach can be considered as an alternative to the outer-inner iteration scheme that does not require multiple restarting procedures.

We address the issue of incompleteness of sounding data when constructing the sequential minimisation algorithm based on the convexification approach. We certainly realise that *a priori* information about the problem has to be used when constructing the algorithm. In general, such an information can be introduced in many ways. For instance, if the sediment characterisation problem is our primary goal, the information about the conductivities of the air, seawater, basement, and the depth $L$ of an inhomogeneous layer is usually available from the direct measurements or geological/geophysical survey. Such an information can be used to construct the three layer support configuration containing the air, seawater and basement layers. It should be pointed out that such a support configuration is not necessarily close in a certain sense to a real configuration. Indeed, the conductivities and thicknesses of sediment layers may differ significantly (up to few times) from the conductivity of the seawater and the depth of water column. Solving analytically the forward problem for the support configuration, one can then simulate the data in a frequency band, which is broader than the actual frequency band available in sounding observations. Extending the actual frequency band, we reduce essentially the approximation errors when constructing the sequential minimisation algorithm. It is proven in this paper that the smaller the approximation error the closer the approximate solution to the "exact" solution of the original inverse problem. Therefore, if sufficiently broad frequency band is available in observations, there is no need for the data extension.

Implementing the convexification approach to EM frequency sounding of layered

conductive media, we exploit the Theorem 5.1 in [1]. However, we do not solve the corresponding minimisation problem for the strictly convex objective function $J_{\lambda,\chi}(q)$ on a compact set $\mathcal{K}(m)$ as indicated in [1]. Instead, we construct its finite-dimensional analog as follows. We divide the interval $[0, L]$ into a finite set of subintervals and approximate the spatial dependence of the transformed field by the quadratic polynomial in each subinterval. The unknown coefficients of these polynomials are the frequency dependent functions. This construction is advantageous for both the error analysis and computational implementation of the algorithm. In the first subinterval, we use the given Dirichlet and Neumann conditions at $z = 0$ in order to express all coefficients via the coefficient of the polynomial leading term. Applying the nonlinear weighted least squares method with Carleman's weight functions, we then formulate a constrained minimisation problem with respect to this coefficient and solve it numerically by the Generalised Reduced Gradient Method (GRGM) (see, e.g., [15]). The proper constraints are obtained from the solution of the forward problem for the support configuration, whereas the starting vector is directly computed from the data. Once the leading coefficient is determined, the transformed field and its first derivative are computed at the right edge of the subinterval. Then they are used in the second subinterval to determine the starting vector. The algorithm is advancing in $[0, L]$ until the last subinterval is met.

Since the transformed field can be determined via the polynomial coefficients, the sequential minimisation algorithm can be viewed as a numerical technique allowing the field continuation in an inhomogeneous lossy layer. In the applied literature, this problem is reffered to as the field prediction. Unlike the traditional layer stripping algorithms (see, e.g., [16], [17]), the sequential minimisation algorithm is stable. The stabilisation is due to Carleman's weight functions that suppress the increase of error in the predicted field when advancing in the interior of an inhomogeneous layer. After the coefficients are computed, the conductivity profile $\sigma(z)$ is determined via the predicted field and data.

Two other globally convergent algorithms for the numerical solution of the inverse scattering problem for the Helmholtz equation in one dimension have been developed. The first algorithm [18] is a certain modification of the stable layer stripping in the frequency domain. The second algorithm [19] exploits causality and the nonlinear Riesz transform and also provides the stability of the layer stripping. However, both these algorithms are applicable to the non-lossy waveguides only.

The paper is arranged as follows. In section 2, the 1-D forward and inverse models of MT shallow sounding are formulated. In section 3, we introduce the concept of sequential minimisation. In section 4, we present the justification of the proposed algorithm and error analysis. Section 5 describes in detail the computational algorithm of sequential minimisation and presents the numerical results. Finally, in section 6, we make conclusions and discuss possible directions for further work.

## 2. Formulations of problems

### *2.1. Forward model*

In MT sounding, the natural sources of the electromagnetic field are used. These sources are mainly due to the solar activity in the ionosphere of the Earth and thunderstorms in its troposphere. Because of remote sources, the EM field varies very slowly in the horizontal directions on Earth's surface allowing one to assume that the EM field in layered media depends on depth. Therefore, we model the distant natural sources by a plane transversely polarised wave normally incident on the surface. For brevity, we consider only the TE-mode of MT sounding assuming that $\mathbf{E} = (E_x, 0, 0)$ and $\mathbf{H} = (0, H_y, H_z)$, where $E_x(z, \tilde{\omega}) = E_0 \exp(i\tilde{\omega}t - k_a z)$ is the $x$-component of the electric field normally incident on the surface $z = 0$, $i = \sqrt{-1}$, $\tilde{\omega}$ is the angular frequency, and $k_a$ is the wavenumber in the air. The TM-mode can be considered by analogy. Under these conditions, the Maxwell's and linear material equations can be reduced in an inhomogeneous layer $[0, L]$ to the scalar equation with respect to the normalised electric field $u(z, \tilde{\omega}) = E_x(z, \tilde{\omega})/E_x(0, \tilde{\omega})$

$$u''(z, \tilde{\omega}) - k^2(z, \tilde{\omega})u(z, \tilde{\omega}) = 0, \ 0 < z < L \tag{2.1}$$

where $u'' = \partial^2 u/\partial z^2$, $k^2(z, \tilde{\omega}) = \tilde{\omega^2}\varepsilon_0\varepsilon\mu(1 + i)\tan\delta(z, \tilde{\omega}))$ is the variable wavenumber, $\tan\delta(z, \tilde{\omega}) = \sigma(z)/\varepsilon_0\varepsilon\tilde{\omega}$ is the loss tangent, and $\sigma(z)$ is the conductivity distribution. Here, the quantities $\varepsilon_0 = 8.85 \cdot 10^{-12}$ $F/m$, $\varepsilon > 0$, and $\mu = 4\pi \cdot 10^{-7}$ $H/m$ are the absolute permettivity of vacuum, the relative permittivity and the magnetic permeability of a medium. The magnetic permeability is assumed to be constant for all layers.

To motivate our further simplifications, we analyse the loss tangent $\tan\delta(z, \tilde{\omega})$. The physical meaning of this quantity can be perceiwed from the representation $k(z, \tilde{\omega}) = \tilde{\omega}(n(z, \tilde{\omega}) + i\kappa(z, \tilde{\omega}))$, where $n$ is the index of refraction characterising the phase speed of an EM wave, and $\kappa$ is the attenuation coefficient characterising the speed of decay of an EM wave amplitude. We have

$$n(z, \tilde{\omega}) = \sqrt{\frac{\varepsilon_0\varepsilon\mu}{2}(\sqrt{1 + \tan^2\delta} + 1)},$$

$$\kappa(z, \tilde{\omega}) = \sqrt{\frac{\varepsilon_0\varepsilon\mu}{2}(\sqrt{1 + \tan^2\delta} - 1)}.$$

It can be seen from these expressions that in the highly conductive media ($\tan\delta \gg 1$), such as marine configurations, $n \approx \kappa = \sqrt{\mu\sigma(z)/\tilde{\omega}}$. This means that both the refraction and attenuation are mainly affected by the conductivity, and the displacement currents are negligibly small at low frequencies. Therefore, we shall neglect the induction current density when considering conductive configurations. Such media cannot be considered in practice as waveguides because of their strong attenuating effect. Quite the reverse, the propagation of the EM field in such media is similar to the diffusion of light in absorbing media. In the case of a poorly conductive media ($\tan\delta \ll 1$), we obtain $n = \sqrt{\varepsilon_0\varepsilon\mu} = const$, $\kappa = \sqrt{\varepsilon_0\varepsilon\mu}\tan\delta/2$. This means that the induction should be taken into account when considering poorly conductive (but lossy!) configurations. Such

conditions are typical when modelling the ground penetrating radar (GPR). In this paper, we restrict our attention to the conductive configurations only. Specifically, the shallow water marine environments (the depth of the water column does not exceed 200 m) are considered.

To derive the boundary conditions for Eq. (2.1), we exploit the continuity of tangential components of both the electric and magnetic fields at $z = 0$ and $z = L$. Since $H_y = (-i\tilde{\omega}\mu)^{-1}\partial E_x/\partial z$, we have two continuity conditions with respect to both $E_x$ and $\partial E_x/\partial z$ at each interface. The surface admittance $Y(\tilde{\omega})$ is defined by

$$Y(\tilde{\omega}) = \frac{H_y(0,\tilde{\omega})}{E_x(0,\tilde{\omega})} = -\frac{1}{i\tilde{\omega}\mu}\frac{E_x'(0,\tilde{\omega})}{E_x(0,\tilde{\omega})} = -\frac{1}{i\tilde{\omega}\mu}u'(0,\tilde{\omega}). \tag{2.2}$$

The depth $L$ is assumed to be known, and the half-space $z > L$ is filled by a homogeneous poorly conductive medium, which we refer to as basement whose conductivity $\sigma_b$ is known. Satisfying the continuity conditions at both interfaces $z = 0$ and $z = L$, we obtain both the Dirichlet $u(0,\tilde{\omega}) = 1$ and Robin $u'(0,\tilde{\omega}) + i\tilde{\omega}\mu Y(\tilde{\omega})u(0,\tilde{\omega}) = 0$ conditions at $z = 0$ and the Robin condition $u'(L,\tilde{\omega}) + k_b u(L,\tilde{\omega}) = 0$ at $z = L$. Here, $u' = \partial u/\partial z$ and $k_b(\tilde{\omega}) = \frac{\sqrt{2}}{2}(i+1)\sqrt{\tilde{\omega}\mu\sigma_b}$. Note that since the transmission field in the half-space $z > L$ is proportional to $\exp(-k_b z)$, the radiation condition as $z \to \infty$ is satisfied. Adding the radiation condition as $z \to -\infty$, we arrive to the forward model that consists of two boundary value problems. The first problem

$$u''(z,\tilde{\omega}) - k_a^2(\tilde{\omega})u(z,\tilde{\omega}) = 0,\ z < 0, \tag{2.3}$$

$$u'(0,\tilde{\omega}) + i\tilde{\omega}\mu Y(\tilde{\omega})u(0,\tilde{\omega}) = 0, \tag{2.4}$$

$$\lim_{z\to-\infty}(u(z,\tilde{\omega}) - \exp(-k_a z)) = 0 \tag{2.5}$$

governs the propagation of the EM field in the homogeneous half space (the air) $z < 0$ with $k_a = \tilde{\omega}\sqrt{\varepsilon_a\varepsilon_0\mu}$. The second boundary value problem

$$u''(z,\tilde{\omega}) - i\mu\tilde{\omega}\sigma(z)u(z,\tilde{\omega}) = 0,\ 0 < z < L, \tag{2.6}$$

$$u(0,\tilde{\omega}) = 1, \tag{2.7}$$

$$u'(L,\tilde{\omega}) + k_b(\tilde{\omega})u(L,\tilde{\omega}) = 0, \tag{2.8}$$

governs the propagation of the EM field in the inhomogeneous layer $0 < z < L$ containing the seawater and sediments. Since the admittance $Y(\tilde{\omega})$ can be determined from the electric and magnetic components of the electromagnetic field measured on the surface as indicated in (2.2), the boundary values problems (2.3)-(2.5) and (2.6)-(2.8) can be separately considered. Since the subject of our investigation is the inhomogeneous layer, we focus on the second problem.

**Lemma 1.** *Let $u \in H^2(0,L)$. Then for any bounded piecewise-continuous function $\sigma(z) \geq const > 0$ and for any $\tilde{\omega} \in [\tilde{\omega}_{min}, \infty)$ the boundary value problem (2.6)-(2.8) is uniquely solvable and its solution $u(z,\tilde{\omega}) \neq 0$ for all $(z,\tilde{\omega}) \in [0,L] \times [\tilde{\omega}_{min}, \infty)$.*

The proof of this lemma is indicated in Appendix B.

For computational reasons, we introduce the dimensionless variables $\xi = z/L$ and $\omega = \tilde{\omega}/\tilde{\omega}_{min}$. Then, the problem (2.6)-(2.8) can be rewritten in the dimensionless form

$$u''(\xi,\omega) - \hat{k}^2(\xi,\omega)u(\xi,\omega) = 0,\ 0 < \xi < 1, \tag{2.9}$$

$$u(0,\omega) = 1, \tag{2.10}$$

$$u(1,\omega) + \hat{k}_b(\omega)u(1,\omega) = 0, \tag{2.11}$$

where $\hat{k}^2(\xi,\omega) = iL^2\tilde{\omega}_{min}\omega\mu\sigma(\xi)$ and $\hat{k}_b(\omega) = \frac{\sqrt{2}}{2}(i+1)L\sqrt{\tilde{\omega}_{min}\omega\mu\sigma_b}$.

### *2.2. Inverse model*

In practice, the horizontal components $E_x$ and $H_y$ of the electromagnetic field are measured on the surface $\xi = 0$. The admittance $Y(\omega)$ and, hence, the vertical gradient $u'(0,\omega) = -i\omega\mu Y(\omega)$ can also be determined from (2.2). The inverse problem of 1-D MT frequency sounding can then be formulated as follows.

**Inverse Problem I**. *Given the function $u'(0,\omega) = \varphi(\omega),\ \omega \in [1,\infty)$, and the normalised electric field satisfies the equations (2.9)-(2.11). Find the conductivity profile $\sigma(\xi),\ \xi \in (0,1)$.*

In practice, the frequency dependence of both components of the electromagnetic field are always measured in the limited frequency band $[1,\omega_{max}]$. For instance, in marine electromagnetics, the upper bound $\omega_{max}/2\pi$ is of the order of hundred Hz. Under these conditions, the formulation given by Inverse Problem I is not consistent with the reality. Therefore, we formulate the following problem.

**Inverse Problem II**. *Given the function $u'(0,\omega) = \varphi(\omega),\ \omega \in [1,\omega_{max}]$, and the normalised electric field satisfies the equations (2.9)-(2.11). Find a certain approximation $\tilde{\sigma}(\xi)$ of the conductivity profile $\sigma(\xi)$.*

*Remark 2.1.* We shall make this formulation more specific in Section 3.2.

## 3. The sequential minimisation algorithm

In the paper [1], it was shown that the Inverse Problem II can be reduced to the problem of minimisation of the strictly convex functional $J_{\lambda,\chi}(p)$ on the compact set $\mathcal{K}(M)$. In this paper, our primary goal is to construct a stable computational algorithm for solving this problem. To achieve this goal, we introduce the concept of sequential minimisation. Specifically, instead minimising the functional $J_{\lambda,\chi}(p)$ on the compact set $\mathcal{K}(M)$, we formulate a finite sequence of more simple minimisation problems and solve them recursively starting from the surface $\xi = 0$ and advancing in the inhomogeneous layer. We apply this concept to the 1-D inverse problem of frequency sounding in four stages: (1) transformations of the original inverse problem to an auxiliary boundary value problem for an integro-differential equation; (2) approximation of the integro-differential operator; (3) the sequential minimisation; (4) inversion of sounding data.

### *3.1. Transformations*

In just the same way as we did before (see [1], Section 4), we introduce the function $w(\xi,\omega) = \ln[u(\xi,\omega)]/\omega$ and transform the problem (2.9) - (2.11) to the following

problem

$$w'' + \omega(w')^2 = i\mu L^2 \tilde{\omega}_{min}\sigma(\xi),\ 0 < \xi < 1, \tag{3.1}$$

$$w(0,\omega) = 0, \tag{3.2}$$

$$w'(0,\omega) = \varphi(\omega)/\omega, \tag{3.3}$$

$$w'(1,\omega) = -\hat{k}_b/\omega, \tag{3.4}$$

where $\varphi(\omega) = u'(0,\omega)$. Next, introducing the function

$$p(\xi,\omega) = \frac{\partial}{\partial\omega}[w(\xi,\omega) - \xi\frac{\varphi(\omega)}{\omega}] \tag{3.5}$$

and using the definition of an antiderivative, i.e., $w(\xi,\omega) - \xi\frac{\varphi(\omega)}{\omega} = -\int_\omega^\infty p(\xi,\nu)d\nu$, we obtain the boundary value problem for an integro-differential equation

$$p'' - 2\omega p' \int_\omega^\infty p'(\xi,\nu)d\nu + (\int_\omega^\infty p'(\xi,\nu)d\nu)^2$$

$$-2\frac{d\varphi(\omega)}{d\omega}\int_\omega^\infty p'(\xi,\nu)d\nu + 2\varphi(\omega)p' - F(\omega) = 0,\ 0 < \xi < 1, \tag{3.6}$$

$$p(0,\omega) = 0, \quad p'(0,\omega) = 0, \tag{3.7}$$

$$p'(1,\omega) = \Psi(\omega), \tag{3.8}$$

where

$$F(\omega) = \frac{\varphi(\omega)}{\omega}[\frac{\varphi(\omega)}{\omega} - 2\frac{d\varphi(\omega)}{d\omega}], \tag{3.9}$$

$$\Psi(\omega) = \frac{1}{\omega}[\frac{\hat{k}_b(\omega) + \varphi(\omega)}{\omega} - \frac{d\hat{k}_b(\omega)}{d\omega} - \frac{d\varphi(\omega)}{d\omega}]. \tag{3.10}$$

We note that the convergence of the integral term in (3.6) was proven in [1]) for the 3-D case. A similar result for the 1-D case is presented in Appendix C. Thus, the Inverse Problem II is reduced to the overdetermined problem (3.6)-(3.10) with respect to the function $p(\xi,\omega)$. One can notice that the latter problem does not contain explicitly the coefficient $\sigma(\xi)$. Instead, it includes the functions $F(\omega)$ and $\Psi(\omega)$ that are determined via the sounding data $\varphi(\omega)$. Since these formal transformations simply scale the normalised field $u(\xi,\omega)$, we observe that the coefficient inverse problem is reduced to the problem of continuation of the scaled electric field from the surface $\xi = 0$ into the inhomogeneous layer. In the applied literature (see, e.g., [8]), such a problem is referred as to the field prediction. Once the field prediction problem is solved, the first and second spatial derivatives of $w(\xi,\omega)$ are computed from the predicted field and, hence, the conductivity distribution is determined from Eq. (3.1).

### *3.2. Approximations*

We first approximate the operator generated by the auxiliary problem (3.6)-(3.10) as follows. Representing the integral of $p'$ as

$$\int_\omega^\infty p'(\xi,\nu)d\nu = \int_\omega^\Omega p'(\xi,\nu)d\nu + \int_\Omega^\infty p'(\xi,\nu)d\nu, \tag{3.11}$$

we rewrite the problem (3.6)-(3.8) in the form

$$L_\Omega(p) - F(\omega) = F_r(\xi, \omega; \Omega),\ 0 < \xi < 1, \tag{3.12}$$

$$p(0,\omega) = 0, \quad p'(0,\omega) = 0, \tag{3.13}$$

$$p'(1,\omega) = \Psi(\omega), \tag{3.14}$$

where

$$L_\Omega(p) \equiv p'' - 2\omega p' \cdot \int_\omega^\Omega p'(\xi,\nu)d\nu + (\int_\omega^\Omega p'(\xi,\nu)d\nu)^2 - 2\frac{d\varphi(\omega)}{d\omega} \cdot \int_\omega^\Omega p'(\xi,\nu)d\nu + 2\varphi(\omega)p', \tag{3.15}$$

and

$$F_r(\xi,\omega;\Omega) = \int_\Omega^\infty p'(\xi,\nu)d\nu \cdot [2\omega p' + 2\frac{d\varphi(\omega)}{d\omega} - 2\int_\omega^\Omega p'(\xi,\nu)d\nu - \int_\Omega^\infty p'(\xi,\nu)d\nu]. \tag{3.16}$$

Let $(a,b) \subseteq (0,1)$ be an arbitrary interval. We define the space

$$C^s_\Omega[a,b] = \{f(\xi,\omega) : f \in C([a,b]\times[1,\Omega]),$$
$$\|f\|_{C^s_\Omega[a,b]} = \max_{j\in[0,s]} \max_{(\xi,\omega)} |\frac{\partial^j}{\partial\xi^j} f(\xi,\omega)| < \infty\},$$

where $s \geq 0$ is an integer number. Since the frequency $\Omega$ is chosen so that the magnitude of the second term in the right-hand side of (3.11) is sufficiently small, it is meaningful to assume that there exists sufficiently small number $\tilde{\varepsilon} > 0$, such that

$$\|F_r\|_{C_\Omega[0,1]} < \tilde{\varepsilon}. \tag{3.17}$$

Therefore, we approximate the problem (3.6)-(3.8) by neglecting the term $F_r(\xi,\omega;\Omega)$. The approximating boundary value problems have the form

$$L_\Omega(p) - F(\omega) = 0,\ 0 < \xi < 1,\ \omega \in [1,\Omega], \tag{3.18}$$

$$p(0,\omega) = 0, \quad p'(0,\omega) = 0, \tag{3.19}$$

$$p'(1,\omega) = \Psi(\omega), \tag{3.20}$$

It should be emphasised that the smallness of the integral $\int_\Omega^\infty p'(\xi,\nu)d\nu$ requires the proper choice of the "cutting" frequency $\Omega$. It would certainly be desirable to take $\Omega = \omega_{max}$. However, it is possible only if sufficiently large upper bound $\omega_{max}$ of the frequency band is available in MT (EM) sounding. Otherwise, the sounding data need to be extended to the interval $(\omega_{max}, \Omega]$ prior to applying the sequential minimisation algorithm. Such an extension provides the appropriately small approximation error and, hence, the small error in the recovered conductivity. If this is the case, we face with the problem of analytic continuation. Indeed, let the domain of the analytic function $\varphi(\omega)$ is $[1,\infty)$. But this function is determined only on the interval $[1,\omega_{max}]$. We wish to find the function $\varphi(\omega)$ in $(\omega_{max},\Omega]$, $\Omega > \omega_{max}$. It is well known that the problem of analytic continuation is, in general, unstable. Although the continuous dependence of the recovered conductivity distribution on perturbations of data is proven in Section 4,

we should take special care when constructing a regularised analytic continuation. The main criterion is to minimise the error of analytic continuation as much as possible. This can be done in several ways. Although a detailed discussion of this problem is outside of the scope of this paper, we indicate in Section 5 one specific procedure for extending the sounding data when dealing with marine configurations. This procedure exploits the support configuration allowing for reducing the approximation error.

Let $u^*$ be the solution of the forward problem (2.9)-(2.11) corresponding to the "exact" conductivity profile $\sigma^*$, such that $\varphi^*(\omega) = u^{*\prime}(0,\omega)$. Since all transformations indicated in Section 3.1 are identical, the function

$$p^*(\xi,\omega) = \frac{\partial}{\partial\omega}[\frac{\ln u^* - \xi\varphi^*}{\omega}]$$

satisfies the conditions (3.12)-(3.14). We formulate the problem of finding a certain approximation of the function $p^*$ as follows.

*Given $\tilde{\varepsilon}$ and the approximate data $\tilde{\varphi}$, such that $\tilde{\varphi} = \varphi^* + \Delta\varphi, \omega \in [1,\Omega]$, $\|\Delta\varphi\|_{C^1[1,\Omega]} \leq \delta$, $\delta > 0$, where $\delta > 0$ and $\tilde{\varepsilon}$ are sufficiently small constants. Find a certain function $\tilde{p}(\xi,\omega)$ close to the function $p^*(\xi,\omega)$, $\{(\xi,\omega) : (\xi,\omega) \in [0,1]\times[1,\Omega]\}$.*

To solve numerically this problem, we construct a least squares solution of the overdetermined problem (3.18)-(3.20) as follows. For each fixed $\omega \in [1,\Omega]$, we first divide the interval $[0,1]$ into $(n-1)$ subintervals

$$0 = \xi_0 < \xi_1 < \xi_2 < ... < \xi_{n-2} < \xi_{n-1} = 1.$$

For brevity, we consider below only an uniform grid. Then we approximate the function $p(\xi,\omega)$ in every subinterval $[\xi_{i-1},\xi_i]$, $(i = 1,2,...,n-1)$ by a quadratic polynomial. The step size $h = 1/(n-1)$ is chosen to be sufficiently small in order to ensure the small error of approximation of the function $p(\xi,\omega)$ by the second degree polynomial. Because of zero Dirichlet and Neumann conditions at $\xi = 0$, we construct the approximation

$$p(\xi,\omega) \approx p_1(\xi,\omega) = \frac{1}{2}a_1(\omega)\xi^2,\ \xi \in (0,\xi_1]. \tag{3.21}$$

Assuming that the function $p_{i-1}(\xi,\omega)$ is known, we derive the recurrence formulae for approximations of $p(\xi,\omega)$ on the subintervals $(\xi_{i-1},\xi_i]$, $(i = 2,3,...,n-2)$

$$\begin{aligned} p(\xi,\omega) &\approx p_i(\xi,\omega) = \frac{1}{2}a_i(\omega)(\xi-\xi_{i-1})^2 \\ &+ p'_{i-1}(\xi_{i-1},\omega)(\xi-\xi_{i-1}) + p_{i-1}(\xi_{i-1},\omega),\ \xi \in (\xi_{i-1},\xi_i]. \end{aligned} \tag{3.22}$$

Taking into account the Neumann condition at $\xi = 1$, we obtain the following approximation on $(\xi_{n-2},\xi_{n-1}]$

$$\begin{aligned} p(\xi,\omega) &\approx p_{n-1}(\xi,\omega) = \frac{1}{2}a_{n-1}(\omega)(\xi-\xi_{n-2})\cdot[(\xi-\xi_{n-2}) - \frac{2}{n}] \\ &+ \Psi(\omega)(\xi-\xi_{n-2}) + p_{n-2}(\xi_{n-2},\omega),\ \xi \in (\xi_{n-2},\xi_{n-1}]. \end{aligned} \tag{3.23}$$

Thus, the function $p(\xi,\omega)$ is approximately determined by the $(n-1)$ unknown coefficients $a_i$, $(i = 1,2,...,n-1)$. This allows us to reduce the nonlinear least squares problem (5.9) from [1] to a sequence of more simple minimisation problems with respect to each $a_i$.

*3.3. Sequential minimisation*

*3.3.1. Constructing the objective functions* Let $M > 0$ be a certain constant. In the space $C^2_\Omega[0,1]$ we consider a convex compact set

$$G(M) = \{g(\xi,\omega) : g \in C^3_\Omega[0,1] : \|g\|_{C^3_\Omega[0,1]} \le M, M > 0\}$$

We also consider in the space $C[1,\Omega]$ a convex bounded set

$$\tilde{G}(M) = \{q(\omega) : q \in C[1,\Omega] : \|q\|_{C[1,\Omega]} \le M\}.$$

By analogy with [1], we consider Carleman's weight functions (CWFs)

$$C_{\lambda,i}(\xi) = \exp\,[-\frac{\lambda}{2}(\xi - \xi_{i-1})], \quad \xi \in [\xi_{i-1}, \xi_i), \tag{3.24}$$

where $\lambda > 0$ is sufficiently large parameter, and a sequence of functionals

$$J_{\lambda,i}(a_i) = \int_1^\Omega \int_{\xi_{i-1}}^{\xi_i} |\hat{L}_\Omega(a_i) - F(\omega)|^2 C^2_{\lambda,i}(\xi) d\xi d\omega, \tag{3.25}$$

where $\hat{L}_\Omega(a_i)$ is the value of the integro-differential operator $L_\Omega(p)$ on the subintervals $[\xi_{i-1}, \xi_i]$ at the function $p(\xi,\omega)$ defined by (3.22), (3.23).

Since both functions $p(\xi_{i-1},\omega)$ and $p'(\xi_{i-1},\omega)$ are known from the preceding iteration, the only function $a_i(\omega)$ is unknown on $[\xi_{i-1}, \xi_i]$.

*3.3.2. The strict convexity of $J_{\lambda,i}$* Before establishing the strict convexity of functionals $J_{\lambda,i}$, we prove two Lemmas. We show first that the CFWs (3.24) provide the Carleman-like estimates for the operator $d^2/d\xi^2$.

**Lemma 2.** *For any complex valued function $u \in H^2(0,l)$, $l = const > 0$, such that $u(0) = u'(0) = 0$, and for any number $\lambda > 0$ the following Carleman-like estimate holds*

$$\int_0^l |u''|^2 \exp\,(-2\lambda x) dx \ge 2\lambda^3 (1+l)^{-2} \int_0^l |u|^2 \exp\,(-2\lambda x) dx. \tag{3.26}$$

*Remark 3.3.2.1.* Unlike the conventional Carleman estimates for the $n$-dimensional Laplace operator (see, e.g., [20], [21]), the estimate (3.26) does not require a zero condition at the right edge $z = l$. On the other hand, we do not use the term

$$\lambda \int_0^l (u')^2 \exp\,(-2\lambda x) dx$$

in the right hand side of the inequality (3.26). This term though can be introduced under assumptions that $u(l) = 0$ and the parameter $\lambda$ is sufficiently large.

*Remark 3.3.2.2.* By virtue of (3.26), the $L_2(0,l)$- weighted norm of the second derivative $u''(x)$ dominates over the same norm of the function $u(x)$ for sufficiently large $\lambda$. This fact is exploited to prove Lemmas 3, 5 and Theorem 1.

**Proof.** Let $u \in H^2(0,l)$ be an arbitrary function satisfying the boundary conditions $u(0) = u'(0) = 0$. Since $u = \Re(u) + i\Im(u)$, we carry out the proof for the real part $\Re(u)$ only. For convenience, we denote $u = \Re(u)$ and $v = u\exp\,(-\lambda x)$. In this case, it is sufficient to assume that $u \in C^2[0,l]$ taking into account that the set $C^2[0,l]$ is dense in $H^2(0,l)$. Then we obtain

$$u' = (v' + \lambda v)\exp\,(\lambda x), \quad u'' = (v'' + 2\lambda v' + \lambda^2 v)\exp\,(\lambda x).$$

Hence,

$$(u'')^2(1+x)^{-1}\exp(-2\lambda x) = [(v^{''}+\lambda v)+2\lambda v']^2(1+x)^{-1}$$
$$\geq 4\lambda v'(v^{''}+\lambda^2 v)(1+x)^{-1} = 2\frac{d}{dx}[(\lambda(v')^2+\lambda^3 v^2(1+x)^{-1})] \quad (3.27)$$
$$+2[\lambda(v')^2+\lambda^3 v^2](1+x)^{-2} \geq 2\lambda^3 u^2(1+x)^{-2}\exp(-2\lambda x)$$
$$+2\frac{d}{dx}[(\lambda(v')^2+\lambda^3 v^2(1+x)^{-1})].$$

Integrating (3.27) with respect to $x$ from 0 to $l$ and taking into account the boundary conditions $u(0)=u'(0)=0$, we obtain

$$\int_0^l (u'')^2(1+x)^{-1}\exp(-2\lambda x)dx \geq 2\lambda^3\int_0^l u^2(1+x)^{-2}\exp(-2\lambda x)dx. \quad (3.28)$$

Since $(1+l)^{-1}\leq(1+x)^{-1}\leq 1$, the inequality (3.28) implies

$$\int_0^l (u'')^2\exp(-2\lambda x)dx \geq \frac{2\lambda^3}{(1+l)^2}\int_0^l u^2\exp(-2\lambda x)dx. \ \square$$

Below $C$ shall denote different positive constants independent of $M,\Omega,\lambda$, and $h$. We also denote $p'_{\imath-1}(\omega)=p'_{\imath-1}(\xi_{\imath-1},\omega),\ p'_0=0$ and

$$I_0(\lambda,h)=\frac{1-\exp(-\lambda h)}{\lambda}=\int_0^h \exp(-\lambda x)dx,\ \lambda>0. \quad (3.29)$$

**Lemma 3.** *Assume that the functions* $\varphi, \frac{d\varphi}{d\omega}\in\tilde{G}(M/2)$ *and* $a_\imath(\omega),\ p_{\imath-1}(\omega),\ p'_{\imath-1}(\omega)\in\tilde{G}(M),\ (\imath=1,...,n-1)$. *Let* $J_{\lambda,\imath}(a_\imath)$ *be the functionals defined by (3.25). Then every functional* $J_{\lambda,\imath}(a_\imath)$ *can be represented in the form*

$$J_{\lambda,\imath}(a_\imath)=I_0(\lambda,h)\cdot[\int_1^\Omega |a_\imath(\omega)-F_\imath(\omega)|^2 d\omega$$
$$+\frac{1}{\lambda}\int_1^\Omega H_\imath(\lambda,\omega)d\omega],\ \forall a_\imath\in\tilde{G}(M),\forall\lambda>1, \quad (3.30)$$

*where*

$$F_\imath(\omega)=F(\omega)+\int_1^\Omega p'_{\imath-1}(\tau)d\tau\cdot[2\omega p'_{\imath-1}(\omega)-\int_1^\Omega p'_{\imath-1}(\tau)d\tau$$
$$+2\frac{d\varphi(\omega)}{d\omega}]-2\varphi p'_{\imath-1}, \quad (3.31)$$

*and the real valued function* $H_\imath$ *satisfies the inequality*

$$\|H_\imath(\lambda,\omega)\|_{C[1,\Omega]}\leq C(M\Omega)^4,\ \forall\lambda\geq 1. \quad (3.32)$$

*Remark 3.3.2.2.* It is proven in Theorem 2 (see Section 4) that the functions $p_{\imath-1}(\omega),\ p'_{\imath-1}(\omega)\in\tilde{G}(M)$.

**Proof.** Let $1\leq\imath\leq n-2$. Taking into account (3.21) and (3.22), we represent the residual $\hat{L}_\Omega(a_\imath)-F$ in the form

$$\hat{L}_\Omega(a_\imath)-F=(a_\imath-F_\imath)(\omega)+(\xi-\xi_{\imath-1})\hat{F}_\imath(a_\imath,\xi-\xi_{\imath-1},\omega) \quad (3.33)$$

where the function $\hat{F}_\imath$ is

$$\hat{F}_\imath(a_\imath,\xi-\xi_{\imath-1},\omega)=\int_1^\Omega a_\imath(\tau)d\tau\cdot[-2\omega(\xi-\xi_{\imath-1})a_\imath-2\omega p'_{\imath-1}$$
$$+(\xi-\xi_{\imath-1})\int_1^\Omega a_\imath(\tau)d\tau-2\frac{d\varphi}{d\omega}]+2\varphi a_\imath. \quad (3.34)$$

It follows from (3.34) that

$$\|\hat{F}_\imath\|_{C^1_\Omega[\xi_{\imath-1},\xi_\imath]} \le C(M\Omega)^2. \tag{3.35}$$

Introduce the moments $I_k$ of CWFs by

$$I_k(\lambda,h) = \int_0^h \xi^k \exp(-\lambda\xi)d\xi,\ (k=1,2). \tag{3.36}$$

Since $I_k = (-1)^k d^k I_0/d\lambda^k$, then it follows from (3.29)

$$\frac{I_k(\lambda,h)}{I_0(\lambda,h)} \le C/\lambda^k,\ (k=1,2),\ \forall\lambda\ge 1. \tag{3.37}$$

Then (3.33)-(3.37) imply (3.30)-(3.32). The case $\imath = n-1$ can be considered by analogy. □

**Theorem 1.** *Let all conditions of Lemma 3 be satisfied, and the functions* $F_\imath \in \tilde{G}(\frac{3}{4}M)$, $(\imath = 1,...,n-1)$. *Then there exists sufficiently large* $\lambda_0 \ge C(\Omega M)^4$, *such that for all* $\lambda \ge \lambda_0$ *every functional* $J_{\lambda,\imath}(a_\imath)$ *is strictly convex on the set* $\tilde{G}(M)$, *i.e.,* $\forall a,b \in \tilde{G}(M)$ *the following inequality holds*

$$J_{\lambda,\imath}(b) - J_{\lambda,\imath}(a) - J'_{\lambda,\imath}(a)(b-a) \ge I_0(\lambda,h)\rho\|a-b\|^2_{L_2(1,\Omega)}, \tag{3.38}$$

*where* $\rho \in (1/2,1)$ *is the parameter of strict convexity independent of* $M,\Omega,\lambda$, *and* $h$ *and* $J'_{\lambda,\imath}$ *is the Frechét derivative of* $J_{\lambda,\imath}$.

**Proof.** Let $1 \le \imath \le n-2$. Let $a(\omega)$ and $b(\omega)$ be two arbirtary functions belonging to the set $\tilde{G}(M)$, $c = b-a$, and

$$q_\imath(\xi,\omega) = \frac{1}{2}b(\omega)(\xi-\xi_{\imath-1})^2 + p'_{\imath-1}(\omega)(\xi-\xi_{\imath-1}) + p_{\imath-1}(\omega).$$

It follows from (3.33) and (3.34) that

$$\begin{aligned} &|\hat{L}_\Omega(q_\imath) - F|^2 = |a+c-F_\imath|^2 \\ &+ 2(\xi-\xi_{\imath-1})\cdot\Re[(a+c-F_\imath)\cdot\overline{\hat{F}}_\imath(a+c,\xi-\xi_{\imath-1},\omega)] \\ &+ (\xi-\xi_{\imath-1})^2\cdot|\hat{F}_\imath(a+c,\xi-\xi_{\imath-1},\omega)|^2, \end{aligned} \tag{3.39}$$

where $\overline{\hat{F}}_\imath$ means the complex conjugate quantity. Then we obtain from (3.34)

$$\begin{aligned} &|\hat{L}_\Omega(q_\imath) - F|^2 = |a-F_\imath|^2 + 2\Re[c(\overline{a}-\overline{F}_\imath)] + |c|^2 \\ &+ (\xi-\xi_{\imath-1})S_1(a,c,\xi-\xi_{\imath-1},\omega) \\ &+ (\xi-\xi_{\imath-1})S_2(a,c,\xi-\xi_{\imath-1},\omega), \end{aligned} \tag{3.40}$$

where $S_1$ and $S_2$ are the linear and nonlinear operators acting on the vector $c = (\Re(c),\Im(c))$. We denote below $\overline{a},\overline{c},\overline{p}'_{\imath-1}$, and $\overline{\varphi}$ the complex conjugate of $a,c,p'_{\imath-1}$, and $\varphi$. The operators $S_1$ and $S_2$ have the forms

$$\begin{aligned} &S_1(a,c,\xi-\xi_{\imath-1},\omega) = 2\Re\{c\cdot\overline{\hat{F}}_\imath(a,\xi-\xi_{\imath-1},\omega) + (a-F_\imath)\times \\ &\{\int_\omega^\Omega \overline{c}\ d\tau[-2(\xi-\xi_{\imath-1})\omega\overline{a} - 2\omega\overline{p}'_{\imath-1} + 2(\xi-\xi_{\imath-1})\int_\omega^\Omega \overline{a}\ d\tau - 2\frac{d\overline{\varphi}}{d\omega}] + 2\overline{\varphi c}\}\} \\ &+2\Re\{\{\int_\omega^\Omega \overline{c}\ d\tau\cdot[-2(\xi-\xi_{\imath-1})\omega a - 2\omega p'_{\imath-1} + 2(\xi-\xi_{\imath-1})\times \\ &\int_\omega^\Omega \overline{a}\ d\tau - 2\frac{d\varphi}{d\omega}] + 2\varphi c\}\cdot\overline{\hat{F}}_\imath(a,\xi-\xi_{\imath-1},\omega)\}, \end{aligned} \tag{3.41}$$

$$S_2(a,c,\xi-\xi_{\imath-1},\omega)=2\Re\{(a-F_\imath)\cdot(\int_\omega^\Omega \overline{c}\ d\tau)^2(\xi-\xi_{\imath-1})$$
$$+c\ \{\int_\omega^\Omega \overline{c}\ d\tau\cdot[-2(\xi-\xi_{\imath-1})\omega\overline{a}-2\omega\overline{p}'_{\imath-1}$$
$$+2(\xi-\xi_{\imath-1})\int_\omega^\Omega \overline{a}d\tau-2\frac{d\overline{\varphi}}{\omega}]+2\overline{\varphi c}+(\int_\omega^\Omega \overline{c}\ d\tau)^2(\xi-\xi_{\imath-1})\}\}$$
$$+2\Re\{(\int_\omega^\Omega c\ d\tau)^2\overline{\hat{F}}_\imath(a,\xi-\xi_{\imath-1},\omega)(\xi-\xi_{\imath-1})\} \tag{3.42}$$
$$+|\int_\omega^\Omega c\ d\tau\cdot[-2(\xi-\xi_{\imath-1})\cdot\omega a-2\omega p'_{\imath-1}+2(\xi-\xi_{\imath-1})\int_\omega^\Omega a\ d\tau-2\frac{d\overline{\varphi}}{\omega}]$$
$$+2\varphi c+(\int_\omega^\Omega c\ d\tau)^2(\xi-\xi_{\imath-1})|^2.$$

From (4.51) and (3.42) we then obtain

$$|\frac{\partial^\jmath}{\partial\xi^\jmath}S_\jmath|\le C(\Omega M)^4,\ \forall a,b\in\tilde{G}(M),\forall c=b-a;\ (\jmath=1,2). \tag{3.43}$$

It follows from (3.36), (3.37), and (3.39)-(3.43) that for all $a,b\in\tilde{G}(M),\ c=b-a,\ \lambda\ge 1$ the following estimate holds

$$J_{\lambda,\imath}(b)-J_{\lambda,\imath}(a)-J'_{\lambda,\imath}(a)(b-a)\ge I_0(\lambda,h)[1+\lambda^{-1}S_3(c,\lambda)]\int_1^\Omega |c|^2d\tau, \tag{3.44}$$

where the functional $S_3(c,\lambda)$ satisfies the inequality

$$|S_3(c,\lambda)|\le C(\Omega M)^4.$$

Choosing the parameter $\lambda$, such that $C(\Omega M)^4\lambda^{-1}\le\gamma,\ \gamma\in(0,1/2)$, we obtain from (3.44)

$$J_{\lambda,\imath}(b)-J_{\lambda,\imath}(a)-J'_{\lambda,\imath}(a)(b-a)\ge I_0(\lambda,h)\cdot[(1-\gamma)\int_1^\Omega |a-b|^2d\tau]. \tag{3.45}$$

The case $\imath=n-1$ can be considered by analogy. □

*3.3.3. The procedure of sequential minimisation* Consider the finite sequence of constrained minimisation problems

$$argmin\{J_{\lambda,\imath}(a_\imath):a_\imath(\omega)\in\tilde{G}(M),(\imath=1,2,...,n-1)\}, \tag{3.46}$$

where

$$J_{\lambda,\imath}(a_\imath)=\int_1^\Omega\int_{\xi_{\imath-1}}^{\xi_\imath}|\hat{L}_\Omega(a_\imath)-F(\omega)|^2C^2_{\lambda,\imath}(\xi)d\xi d\omega. \tag{3.47}$$

These problems (3.46) can only be recursively solved. Introducing the functions $\rho_\imath(\xi),\eta_\imath(\xi,\omega)$

$$\rho_\imath(\xi)=\begin{cases}\xi,\ \ \xi\in[\xi_0,\xi_1]\\ \xi-\xi_{\imath-1},\ \ \xi\in(\xi_{\imath-1},\xi_\imath],\ (\imath=2,...,n-2)\\ (\xi-\xi_{n-2})-1/n,\ \ \xi\in(\xi_{n-2},\xi_{n-1}],\end{cases} \tag{3.48}$$

$$\eta_\imath(\xi,\omega)=\begin{cases}0,\ \ \xi\in[\xi_0,\xi_1]\\ p'_{\imath-1}(\xi_{\imath-1},\omega),\ \ \xi\in(\xi_{\imath-1},\xi_\imath],\ (\imath=2,...,n-2)\\ \Psi(\omega),\ \ \xi\in(\xi_{n-2},\xi_{n-1}],\end{cases} \tag{3.49}$$

we obtain

$$\hat{L}_\Omega(a_\imath) = a_\imath - 2\omega(a_\imath\rho_\imath^2+\eta_\imath)\int_\omega^\Omega a_\imath(\nu)d\nu - 2\omega(a_\imath\rho_\imath^2+\eta_\imath)\int_\omega^\Omega \eta_\imath(\xi,\nu)d\nu$$
$$+\rho_\imath^2(\int_\omega^\Omega a_\imath(\nu)d\nu)^2 + (\int_\omega^\Omega \eta_\imath(\xi,\nu)d\nu)^2 + 2\rho_\imath\int_\omega^\Omega a_\imath(\nu)d\nu\int_\omega^\Omega \eta_\imath(\xi,\nu)d\nu$$
$$-2\frac{d\varphi}{d\omega}\rho_\imath\int_\omega^\Omega a_\imath(\nu)d\nu - 2\frac{d\varphi}{d\omega}\int_\omega^\Omega \eta_\imath(\xi,\nu)d\nu + 2\varphi\rho_\imath a_\imath + 2\varphi\eta_\imath. \tag{3.50}$$

Since the functions $\eta_\imath(\xi,\omega)$ are recursively computed, the operators $\hat{L}_\Omega(a_\imath)$ and functionals $J_{\lambda\imath}(a_\imath)$ are recursively found as well. This feature motivates the term "the sequential minimisation". Specifically, we first solve numerically the constrained minimisation problem (3.46) for $\imath = 1$ computing the approximate minimiser $\tilde{a}_1$. We then use the expression (3.21) to calculate the approximations of $p_1(\xi_1,\omega)$ and $p_1'(\xi_1,\omega)$ and, hence, compute $\hat{L}_\Omega(a_2)$, $J_{\lambda,\imath}(a_2)$ and the minimiser $\tilde{a}_2$, etc. until the last minimiser $\tilde{a}_{n-1}$ is computed. Note that the expressions (3.22) and (3.23) are used to calculate the approximations of $p_\imath'(\xi_\imath,\omega)$ for $\imath = 2,...,n-1$. We prove below that all minimisers $\tilde{a}_\imath$ are the interior points of the set $\tilde{G}(M)$. Therefore, they are uniquely determined due to the strict convexity of functionals $J_{\lambda,\imath}(a_\imath)$. In Section 5.3, we discuss some details of implementation of this procedure.

### *3.4. Inversion*

Once the minimisers $\tilde{a}_\imath(\omega)$ are found, the approximate first and second derivatives of the predicted field $\tilde{p}(\xi,\omega)$ are determined as

$$\tilde{p}'(\xi,\omega) = \begin{cases} \tilde{a}_1(\omega)\xi, & \xi\in[\xi_0,\xi_1] \\ \tilde{a}_\imath(\omega)(\xi-\xi_{\imath-1}) + \tilde{p}'_{\imath-1}, & \xi\in(\xi_{\imath-1},\xi_\imath],\ (\imath=2,...,n-2) \\ \tilde{a}_{n-1}(\omega)[(\xi-\xi_{n-2})-1/n] + \Psi(\omega), & \xi\in(\xi_{n-2},\xi_{n-1}], \end{cases} \tag{3.51}$$

$$\tilde{p}''(\xi,\omega) = \begin{cases} \tilde{a}_1(\omega), & \xi\in[\xi_0,\xi_1] \\ \tilde{a}_\imath(\omega), & \xi\in(\xi_{\imath-1},\xi_\imath],\ (\imath=2,...,n-1). \end{cases} \tag{3.52}$$

These approximate derivatives can be used to determine the approximate conductivity. Indeed, it has been indicated in Section 3.1 that

$$w(\xi,\omega) = -\int_\omega^\infty p(\xi,\nu)d\nu + \xi\frac{\varphi(\omega)}{\omega} = -\int_\omega^\Omega p(\xi,\nu)d\nu - \int_\Omega^\infty p(\xi,\nu)d\nu + \xi\frac{\varphi(\omega)}{\omega}$$
$$= -\int_\omega^\Omega p(\xi,\nu)d\nu + w(\xi,\Omega) + \xi\frac{\varphi(\omega)}{\omega}.$$

If the frequency $\Omega$ is sufficiently large, the functions $w(\xi,\Omega)$, $w'(\xi,\Omega)$, and $w''(\xi,\Omega)$ are small. Therefore, we may approximate the functions $w'$ and $w''$ by

$$\tilde{w}'(\xi,\omega) = -\int_\omega^\Omega \tilde{p}'(\xi,\nu)d\nu + \frac{\varphi(\omega)}{\omega} + w_s'(\xi,\Omega), \tag{3.53}$$

$$\tilde{w}''(\xi,\omega) = -\int_\omega^\Omega \tilde{p}''(\xi,\nu)d\nu + w_s''(\xi,\Omega), \tag{3.54}$$

where $w_s(\xi,\Omega)$ is the $w$-field at the frequency $\Omega$ for the support configuration (see Section 5.1), which is known. Since the right-hand side of Eq. (3.1) does not depend

on $\omega$, its left-hand side, i.e., the expression $w'' + \omega(w')^2$, does not depend on $\omega$ as well. In principle, one can choose a certain fixed frequency $\omega \in [1, \Omega)$ in (3.53) - (3.54) when solving Eq. (3.1) with respect to $\sigma(\xi)$. To reduce the approximation error, we however choose $\omega = 1$. Then we obtain the explicit formula for the solution of Inverse Problem II

$$\tilde{\sigma}(\xi) = \frac{1}{\mu L^2 \tilde{\omega}_{min}}[2\alpha_\imath \Re(I_\imath)\Im(I_\imath) + \Re(\beta_\imath)\Im(I_\imath) + \Re(I_\imath)\Im(\beta_\imath) + \Im(\gamma_\imath)], \quad (3.55)$$

where

$$I_\imath = -\int_1^\Omega a_\imath(\nu)d\nu, \quad (3.56)$$

$$\begin{aligned} \alpha_\imath &= \omega\rho_\imath^2(\xi), \\ \beta_\imath &= 1 + 2\omega\tau_\imath(\xi)\rho_\imath(\xi), \\ \gamma_\imath &= \omega\tau_\imath^2(\xi), \end{aligned} \quad (3.57)$$

and

$$\tau_\imath(\xi) = \begin{cases} \varphi(1), \quad \xi \in [\xi_0, \xi_1] \\ \varphi(1) + \int_1^\Omega p'_{\imath-1}d\nu, \quad \xi \in (\xi_{\imath-1}, \xi_\imath], \ (\imath = 2, ..., n-2) \\ \varphi(1) + \int_1^\Omega \Psi d\nu, \quad \xi \in (\xi_{n-2}, \xi_{n-1}]. \end{cases} \quad (3.58)$$

## 4. Error estimates

In Section 3.2, we have introduced the function $p^*$ corresponding to the "exact" solution $\sigma^*$ of Inverse Problem I. However, the sequential minimisation algorithm results in a certain function $\tilde{p}$ that generates the solution $\tilde{\sigma}$ of Inverse Problem II. It is clear that $\tilde{\varepsilon} \to 0$ as $\Omega \to \infty$. In practice, both the parameters $\tilde{\varepsilon}$ and $\delta$ and the frequency $\Omega$ may vary in broad ranges. Under these conditions, the sequential minimisation algorithm requires the stability analysis. In other words, the continuous dependence of a certain norm $\|\tilde{p} - p^*\|$ on $\delta$, $\tilde{\varepsilon}$, and the step size $h$ must be rigorously justified. In this Section, we establish such a dependence. We first prove three Lemmas.

**Lemma 4.** *For any complex valued function $s \in C[1, \Omega]$, the Frechét derivative of the functional $J_{\lambda,\imath}(a_\imath)$, $(\imath = 1, 2, ..., n-2)$ is given by*

$$\begin{aligned} &J'_{\lambda,\imath}(a_\imath)(s) = I_0(\lambda, h) \cdot 2\Re[\int_1^\Omega \overline{s}(\omega)(a_\imath - F_\imath)d\omega] \\ &+2\Re\{\int_1^\Omega s(\omega)(1 + 2\varphi(\omega)) \cdot \int_{\xi_{\imath-1}}^{\xi_\imath} (\xi - \xi_{\imath-1})C^2_{\lambda,\imath}(\xi) \\ &\times\{\int_\omega^\Omega \overline{a}_\imath(\tau)d\tau[-2(\xi - \xi_{\imath-1})\omega\overline{a}_\imath - 2\omega p'_{\imath-1} \\ &+(\xi - \xi_{\imath 1})\int_\omega^\Omega \overline{a}_\imath(\tau)d\tau - 2\frac{d\overline{\varphi}}{d\omega}] + 2\overline{\varphi a}_\imath\}d\xi d\omega\} \\ &+2\Re\{\int_1^\Omega s(\omega)\int_{\xi_{\imath-1}}^{\xi_\imath} (\xi - \xi_{\imath-1})C^2_{\lambda,\imath}(\xi) \\ &\times\int_1^\omega d\tau\{(\overline{a}_\imath - \overline{F}_\imath)[-2(\xi - \xi_{\imath-1})\tau\overline{a}_\imath - 2\tau p'_{\imath-1} \end{aligned}$$

$$+2(\xi-\xi_{\imath-1})\int_\tau^\Omega a_\imath(\nu)d\nu-2\frac{d\varphi}{d\omega}]\}d\xi d\omega\}$$
$$+2\Re\{\int_1^\Omega s(\omega)\int_{\xi_{\imath-1}}^{\xi_\imath}(\xi-\xi_{\imath-1})C^2_{\lambda,\imath}(\xi)$$
$$\times\int_1^\omega d\tau\{[-2(\xi-\xi_{\imath-1})\tau\overline{a}_\imath-2\tau p'_{\imath-1}$$
$$+2(\xi-\xi_{\imath-1})\int_\tau^\Omega a_\imath(\nu)d\nu-2\frac{d\varphi}{d\omega}]\cdot\overline{\hat{F}}(a_\imath,\xi-\xi_{\imath-1},\tau)\}d\xi d\omega\},$$

*where* $\overline{\hat{F}}$ *is defined by (3.34).*

**Proof.** It follows from (3.25), (3.40), and (3.41). □

*Remark 4.1.* The analogous formula for $J_{\lambda,(n-1)}(a_{n-1})$ can be obtained in the same way.

**Lemma 5.** *Suppose the functions* $\varphi, \frac{d\varphi}{d\omega}\in\tilde{G}(M/2)$ *and* $p'_{\imath-1}\in\tilde{G}(M)$, $F_\imath\in\tilde{G}(\frac{3}{4}M)$. *Then there exists sufficiently large number* $\lambda_0\geq C(\Omega M)^4$, *such that the functional* $J_{\lambda,\imath}(a_\imath)$ *is strictly convex on the set* $\tilde{G}(M)$ *for all* $\lambda\geq\lambda_0$ *and for each* $1\leq\imath\leq n-1$, *the minimisation problem*

$$argmin\{J_{\lambda,\imath}(a_\imath):a_\imath\in\tilde{G}(M)\} \tag{4.1}$$

*is uniquely solvable, and the minimiser* $\tilde{a}_\imath$ *is an interior point of* $\tilde{G}(M)$.

**Proof.** It follows from Theorem 1 that the functional $J_{\imath,\lambda}(a_\imath)$ is strictly convex on the set $\tilde{G}(M)$. Therefore, it is sufficient to show that for sufficiently large $\lambda\geq\lambda_0\geq C(M\Omega)^4$ the equation

$$J'_{\lambda,\imath}(a_\imath)(s)=0,\ \forall s\in\tilde{G}(M) \tag{4.2}$$

has a unique solution belonging to the interior of $\tilde{G}(M)$. Let $1\leq\imath\leq n-2$. It follows from (3.31) that $F_1=F$. Lemma 4, (3.29), (3.36), and (3.37) imply that for any complex valued function $s\in C[1,\Omega]$ the following equality holds

$$J'_{\lambda,\imath}(a_\imath)(s)=I_0(\lambda,h)\cdot[2\Re\int_1^\Omega s(\omega)(\overline{a}_\imath-\overline{F}_\imath)d\omega$$
$$-2\Re\int_1^\Omega s(\omega)\cdot\lambda^{-1}T_\imath(a_\imath,\omega,\lambda)d\omega], \tag{4.3}$$

where

$$\|T_\imath(a_\imath,\omega,\lambda)\|_{C[1,\Omega]}\leq C(\Omega M)^2,\ \forall a_\imath\in\tilde{G}(M),\ \forall\lambda\geq\lambda_0. \tag{4.4}$$

We obtain from (4.2) and (4.3) the equivalent equation

$$a_\imath(\omega)=F_\imath+\lambda^{-1}\overline{T}_\imath(a_\imath,\omega,\lambda). \tag{4.5}$$

Define the map $A_\imath:C[1,\Omega]\to C[1,\Omega]$ by

$$A_\imath(a)=F_\imath+\lambda^{-1}\overline{T}_\imath(a,\omega,\lambda). \tag{4.6}$$

We can then rewrite Eq. (4.5) in the form

$$a_\imath=A_\imath(a_\imath). \tag{4.7}$$

Choose $\lambda_0\geq C(\Omega M)^4$, such that the following inequality holds

$$\lambda^{-1}C(\Omega M)^2<M/4. \tag{4.8}$$

Since $F_\imath \in \tilde{G}(\frac{3}{4}M)$, we obtain from (4.4)-(4.8)

$$\|A_\imath(a_\imath)\|_{C[1,\Omega]} \leq \|F_\imath\|_{C[1,\Omega]} + \frac{M}{4} < \frac{3}{4}M + \frac{M}{4} < M. \tag{4.9}$$

This inequality implies that

$$A_\imath : \tilde{G}(M) \to \tilde{G}(M). \tag{4.10}$$

It follows from Lemma 4 and (4.3) that

$$\begin{aligned}\|A_\imath(a_1) - A_\imath(a_2)\|_{C[1,\Omega]} &\leq \lambda^{-1}\|T_\imath(a_1,\omega,\lambda) - T_\imath(a_2,\omega,\lambda)\|_{C[1,\Omega]} \\ &\leq \lambda^{-1}C(\Omega M)^2\|a_1 - a_2\|_{C[1,\Omega]},\ \forall a_1, a_2 \in \tilde{G}_\imath(M).\end{aligned} \tag{4.11}$$

In addition to (4.8), choose sufficiently large parameter $\lambda_0$, so that for $\lambda \geq \lambda_0$

$$\lambda^{-1}C(\Omega M)^2 < 1/2. \tag{4.12}$$

Then the equations (4.10)-(4.12) imply that the map $A_\imath$ is contractive on the set $\tilde{G}(M)$. The case $\imath = n-1$ can be considered by analogy. $\square$

Remembering (see Section 3.2) that the function $\varphi^*(\omega)$ corresponds to the "exact" conductivity distribution $\sigma^*(\xi)$, we shall call $\varphi^*(\omega)$ the "exact" sounding data. Also, we denote

$$F^*(\omega) = \frac{\varphi^*(\omega)}{\omega} \cdot [\frac{\varphi^*(\omega)}{\omega} - 2\frac{d\varphi^*(\omega)}{d\omega}], \tag{4.13}$$

$$\begin{aligned}L^*_\Omega(p^*,\varphi^*) &= p^{*\prime\prime} - 2\omega p^{*\prime}\int_\omega^\Omega p^{*\prime}d\tau + (\int_\omega^\Omega p^{*\prime}d\tau)^2 \\ &-2\frac{d\varphi^*(\omega)}{d\omega}\int_\omega^\Omega p^{*\prime}d\tau + 2\varphi^* p^{*\prime},\end{aligned} \tag{4.14}$$

$$\Delta F = F - F^*,\ \Delta\varphi = \varphi - \varphi*. \tag{4.15}$$

By analogy with (3.31), we denote

$$\begin{aligned}F^*_\imath(\omega) = F^*(\omega) &+ \int_1^\Omega p^{*\prime}_{\imath-1}(\tau)d\tau \cdot [2\omega p^{*\prime}_{\imath-1}(\omega) - \int_1^\Omega p^{*\prime}_{\imath-1}(\tau)d\tau \\ &+ 2\frac{d\varphi^*(\omega)}{d\omega}] - 2\varphi^* p^{*\prime}_{\imath-1}.\end{aligned} \tag{4.16}$$

Then, we have $F^*_1 = F^*$. Furthermore, let us denote $\varepsilon = |(\tilde{\varepsilon},\delta)|$. Without loss of generality, assume that the following inequalities are fulfilled

$$\|\Delta F\|_{C[1,\Omega]} < \frac{\varepsilon}{4}, \tag{4.17}$$

$$\|L^*_\Omega(p^*,\varphi^*) - F^*\|_{C[1,\Omega]} < \frac{\varepsilon}{4}, \tag{4.18}$$

$$\|\Delta\varphi\|_{C^1[1,\Omega]} < \frac{\varepsilon}{4}. \tag{4.19}$$

Also, denote $(p^*_{\imath-1})^{(s)}(\omega) = (p^*_{\imath-1})^{(s)}(\xi_{\imath-1},\omega),\ s = 1,2;\ 1 \leq \imath \leq n$.

**Lemma 6** *Let $p^* \in G(M/2)$ and the inequalities (4.17)-(4.19) hold. Then the following inequality holds*

$$\|F^*_\imath\|_{C[1,\Omega]} \leq \frac{M}{2} + \frac{\varepsilon}{4},\ (\imath = 1,...,n-1). \tag{4.20}$$

**Proof.** Let $1 \le \imath \le n-2$. We have from (4.14) and (4.16)

$$L^*_\Omega(p^*(\xi_{\imath-1},\omega),\varphi^*) - F^*(\omega) = (p^*_{\imath-1})''(\omega) - F^*_\imath(\omega). \tag{4.21}$$

The inequality (4.18) implies that $\|F^*_\imath\|_{C[1,\Omega]} \le \varepsilon/4 + \|(p^*)''_{\imath-1}\|_{C[1,\Omega]}$. Since $p^* \in G(M/2)$, we obtain the inequality (4.20) from (4.21). The case $\imath = n-1$ can be considered by analogy. □

**Theorem 2** *Let $\sigma^*(\xi) \ge const > 0$ be a bounded piecewise continuous function on $[0,1]$, $p^* \in G(M/2)$, and the inequalities (4.17)-(4.19) hold. Let $\lambda_0 \ge C(\Omega M)^4$ be sufficiently large parameter, such that for $\lambda \ge \lambda_0$ the inequalities (4.8) and (4.12) hold and*

$$\lambda^{-1} C(\Omega M)^2 < \frac{\varepsilon}{2}, \tag{4.22}$$

*For such $\lambda$, let $\{\tilde{p}_\imath(\xi,\omega)\}_{\imath=1}^{\imath=n}$ be the sequence of functions corresponding to the coefficients $\tilde{a}_\imath$ determined via the procedure of sequential minimisation, i.e., the functions $\tilde{p}_\imath(\xi,\omega)$ are determined from Eqs (3.22), (3.23). Then there exist sufficiently small numbers $\varepsilon_0 = \varepsilon_0(\Omega,M) > 0, h_0 = h_0(\Omega,M) > 0$, such that for all $\varepsilon \in (0,\varepsilon_0)$, $h \in (0,h_0)$ the functions*

$$\tilde{p}'_{\imath-1}(\xi_{\imath-1},\omega)\ \tilde{p}''_{\imath-1}(\xi_{\imath-1},\omega) \in \tilde{G}(M),\ (\imath = 1,...,n-1), \tag{4.23}$$

$$F_\imath \in \tilde{G}(\frac{3}{4}M),\ (\imath = 1,...,n-1) \tag{4.24}$$

*and the following estimates hold*

$$\|\Delta p^{(s)}_\imath\|_{C[1,\Omega]} \le K(\varepsilon + h),\ (s = 0,1,2),\ (\imath = 1,...,n-1), \tag{4.25}$$

*where*

$$\Delta p^{(s)}_\imath(\omega) = \frac{\partial^{(s)}}{\partial \xi^{(s)}}[\tilde{p}_\imath(\xi_{\imath-1},\omega) - p^*(\xi_{\imath-1},\omega)], \tag{4.26}$$

*$\tilde{p}_0(\xi_0,\omega) = \tilde{p'}_0(\xi_0,\omega) = 0$, $\tilde{p''}_0(\xi_0,\omega) = \tilde{a}_1(\omega)$, and $K = K(\Omega,M) > 0$ is a constant depending on $\Omega$ and $M$. But it does not depend on $\varepsilon$, $\lambda$, and $h$.*

*Remark 4.2.* It follows from Lemma 5 and Theorem 2 that $\tilde{G}(M)$ is a correctness set for the minimisation problems (3.46)-(3.47). This means that these problems are conditionally well-posed on $\tilde{G}(M)$ according to the concepts and definitions indicated in [20], [22], [23]. In other words, the specific forms of the objective functions $J_{\lambda,\imath}(a_\imath)$ and the feasible region $\tilde{G}(M)$ for unknowns $a_\imath(\omega)$ allow us to regularise the originally ill-posed $p$-field prediction problem.

*Remark 4.3.* Without loss of generality, we assume below that $\Omega \ge 1, M \ge 1$.

**Proof.** In this proof we assume that $\|\cdot\| = \|\cdot\|_{C[1,\Omega]}$. The mathematical induction is used to prove the theorem. Let $\imath = 1$. Then we obtain from (3.21)

$$p_1 = a_1(\omega)\frac{\xi^2}{2},\ \xi \in (\xi_0,\xi_1].$$

Since $F^*_1 = F^*$, we have from (4.17) and (4.18)

$$\|F_1\| < \frac{(M+\varepsilon)}{2} < \frac{3}{4}M,$$

where $F_1 = F$ and $\varepsilon < \varepsilon_0 < M/2$. This means that $F_1 \in \tilde{G}(3M/4)$. This fact proves (4.24) for $\imath = 1$. It follows from Theorem 1 and Lemma 5 that the functional $J_{\lambda,1}$ is strictly convex on $\tilde{G}(M)$ and its unique minimiser $\tilde{a}_1$ belongs to the interior of $\tilde{G}(M)$. On the other hand, due to (4.5), this minimiser is the unique solution of the equation

$$\tilde{a}_1(\omega) = F_1 + \lambda^{-1}\overline{T}_1(\tilde{a}_1, \omega, \lambda). \tag{4.27}$$

Denote $g^*_\varepsilon(\xi, \omega) = L_\Omega(p^*, \varphi^*) - F^*$. Then, we have from (4.18)

$$\|g^*_\varepsilon(\xi, \omega)\|_{C_\Omega[0,1]} < \frac{\varepsilon}{4}. \tag{4.28}$$

From (4.21), we have $(p^*_0)'' = F^*_1 + g^*_\varepsilon(0, \omega)$. Using Taylor's formula, we obtain

$$p^*(\xi, \omega) = a^*_1(\omega)\frac{\xi^2}{2} + \frac{1}{2}\int_0^\xi (\xi - \xi')^2 p^{*(3)}(\xi', \omega)d\xi',\ \xi \in (\xi_0, \xi_1), \tag{4.29}$$

where $a^*_1 = F^*_1 + g^*_\varepsilon(0, \omega)$. Denoting $\Delta a_1 = \tilde{a}_1 - a^*_1$ and $\Delta F_1 = F_1 - F^*$, we obtain from (4.27)

$$\Delta a_1 = \Delta F_1 + \lambda^{-1}\overline{T}_1(\tilde{a}_1, \omega, \lambda) - g^*_\varepsilon(0, \omega). \tag{4.30}$$

We have from (4.4), (4.17), (4.22), (4.28), and (4.30)

$$\|\Delta a_1\| \le \frac{\varepsilon}{4} + \frac{\varepsilon}{2} + \frac{\varepsilon}{4} = \varepsilon. \tag{4.31}$$

Using (4.29) and (4.31), we obtain

$$\Delta p'_2 = (p'_1 - p^{*\prime})(\xi_1, \omega) = \Delta a_1 \cdot h - \int_0^h (h - \xi')p^{*(3)}(\xi', \omega)d\xi'.$$

Since $p^* \in G(M/2)$, we then obtain from (4.31)

$$\|\Delta p'_2\| \le \varepsilon h + Mh^2/4. \tag{4.32}$$

Noticing that $\Delta p_2 = \Delta a_1 \cdot h^2/2 + \Delta p'_2 \cdot h$, we obtain from (4.31) and (4.32)

$$\|\Delta p_2\| \le \frac{3}{2}\varepsilon h^2 + Mh^3/4. \tag{4.33}$$

The estimate (4.25) for $\imath = 2$ follows immediately from (4.26), (4.31), (4.32) and (4.33). For $\imath = 1$, it is obvious since $\Delta p_1 = \Delta p'_1 = 0,\ \Delta p''_1 = \Delta a_1$, and (4.31) holds.

Since $p'_1(\xi_1, \omega) = \Delta p'_2(\omega) + p^{*\prime}(\xi_1, \omega)$ and $p^* \in G(M/2)$, then (4.32) implies

$$\|p'_1\| \le \frac{M}{2} + \varepsilon h + \frac{M}{4}h^2. \tag{4.34}$$

Also, it follows from (4.31) that

$$\|a_1\| < \frac{M}{2} + \varepsilon. \tag{4.35}$$

Assume that the following inequalities hold

$$\varepsilon h + \frac{M}{4}h^2 < \frac{M}{2},\ \forall (\varepsilon, h) \in (0, \varepsilon_0) \times (0, h_0), \tag{4.36}$$

$$\varepsilon < \frac{M}{2},\ \forall \varepsilon \in (0, \varepsilon_0) \subset (0, 1). \tag{4.37}$$

Then, the inequalities (4.34) and (4.35) imply

$$\tilde{p'}_1(\xi_1, \omega),\ \tilde{p''}_1(\xi_1, \omega) \in \tilde{G}(M). \tag{4.38}$$

Since $\tilde{p'}_1(\xi_0,\omega) = 0$, $\tilde{p''}_0(\xi_0,\omega) = \tilde{a}_1(\omega)$, then (4.38) establishes (4.23) for $\imath = 1,2$. To prove (4.24) for $\imath = 2$, consider the quantity $\Delta F_\imath = F_\imath - F_\imath^*$. By virtue of (3.31) and (4.16), we have

$$\begin{aligned}\Delta F_\imath = \Delta F_1 &+ \int_\omega^\Omega \Delta p'_\imath(\tau)d\tau \cdot [2\omega p^{*'}_{\imath-1}(\omega) - \int_\omega^\Omega p^{*'}_{\imath-1}(\tau)d\tau + 2\frac{d\varphi^*}{d\omega}] \\ &+ \int_\omega^\Omega \tilde{p'}_{\imath-1}(\tau)d\tau \cdot [2\omega\Delta p'_\imath - \int_\omega^\Omega \Delta p'_{\imath-1}(\tau)d\tau + 2\Delta\frac{d\varphi}{d\omega}] \\ &- 2\Delta\varphi \cdot p^{*'}_{\imath-1} - 2\varphi\Delta p_\imath. \end{aligned} \tag{4.39}$$

Assuming $\imath = 2$ in (4.39) and taking account of (4.17), (4.19), (4.32) and (4.38), we obtain

$$\begin{aligned}\|\Delta F_2\| &\le \frac{\varepsilon}{4}(1 + 2\Omega M + M) + \|\Delta p'_2\| \cdot (5\Omega^2 M + 3M) \\ &\le 8\Omega^2 M(\varepsilon + \varepsilon h + Mh^2).\end{aligned}$$

Applying (4.20), we obtain

$$\|F_2\| \le \frac{M}{2} + \frac{\varepsilon}{4} + 8\Omega^2 M(\varepsilon + \varepsilon h + Mh^2). \tag{4.40}$$

Assume that in addition to (4.36) and (4.37), the following inequality holds

$$\frac{\varepsilon}{4} + 8\Omega^2 M(\varepsilon + \varepsilon h + Mh^2) < \frac{M}{5},\ \forall(\varepsilon,h) \in (0,\varepsilon_0) \times (0,h_0). \tag{4.41}$$

Then the inequality (4.40) implies $\|F_2\| < M/2 + M/5 < 3M/4$, which establishes (4.24) for $\imath = 2$.

Let $2 \le k \le n-2$. Assume that (4.23) hold for $1 \le \jmath \le k-1$ and (4.24), (4.25) hold for $1 \le \jmath \le k$ and $s = 1,2$. We shall establish (4.23) for $\jmath = k$ and (4.24), (4.25) for $\jmath = k+1$.

It follows from Theorem 1 that the functional $J_{\lambda,k}(a_k)$ is strictly convex on the set $\tilde{G}(M)$. Also, it follows from Lemma 5 and (4.5) that its unique minimiser belonging to the interior of $\tilde{G}(M)$ satisfies the equation

$$\tilde{a}_k(\omega) = F_k(\omega) + \lambda^{-1}\overline{T}_k(\tilde{a}_k,\omega,\lambda). \tag{4.42}$$

Representing the function $p^*(\xi,\omega)$ via Taylor's formula, we obtain

$$\begin{aligned}p^*(\xi,\omega) = a_k^*(\omega)\frac{(\xi-\xi_{k-1})^2}{2} &+ p^{*'}(\xi_{k-1},\omega)(\xi-\xi_{k-1}) + p^*(\xi_{k-1},\omega) \\ &+ \frac{1}{2}\int_{\xi_{k-1}}^{\xi}(\xi-\xi')^2 p^{*(3)}(\xi',\omega)d\xi',\ \xi \in (\xi_{k-1},\xi_k).\end{aligned} \tag{4.43}$$

Therefore, the equations (4.14) and (4.16) imply

$$a_k^*(\omega) = p^{*''}(\xi_{k-1},\omega) = g_\varepsilon^*(\xi_{k-1},\omega) + F_k^*(\omega). \tag{4.44}$$

Subtracting (4.44) from (4.42) and denoting $\Delta a_k = \tilde{a}_k - a_k^*$, we obtain

$$\Delta a_k = \Delta F_k + \lambda^{-1}\overline{T}_k(\tilde{a}_k,\omega,\lambda) - g_\varepsilon^*(\xi_{k-1},\omega). \tag{4.45}$$

It follows from (4.4), (4.22), and (4.28) that

$$\|\Delta a_k\| \le \|\Delta F_k\| + \frac{\varepsilon}{2} + \frac{\varepsilon}{4} \le \|\Delta F_k\| + \frac{3}{4}\varepsilon. \tag{4.46}$$

From (4.17), (4.19), and (4.39) we obtain

$$\|\Delta F_k\| \le (2\Omega M)\cdot\varepsilon + 9(\Omega^2 M)\cdot\|\Delta p'_k\|. \tag{4.47}$$

Hence, the inequality (4.46) implies

$$\|\Delta a_k\| \le (3\Omega M)\cdot\varepsilon + 9(\Omega^2 M)\cdot\|\Delta p'_k\|. \tag{4.48}$$

It follows from (3.22) that $\tilde{p}'_k(\xi_k,\omega) = \tilde{a}_k\cdot h + \tilde{p}'_{k-1}(\xi_{k-1},\omega)$. Hence, the equations (4.26), (4.43) imply

$$\Delta p'_{k+1} = \Delta a_k\cdot h + \Delta p'_k - \int_{\xi_{k-1}}^{\xi_k}(\xi_k-\xi')p^{*(3)}(\xi',\omega)d\xi',$$

$$\|\Delta p'_{k+1}\| \le \|\Delta a_k\|\cdot h + \|\Delta p'_k\| + \frac{Mh^2}{4}.$$

Taking into account (4.48), we then obtain

$$\|\Delta p'_{k+1}\| \le (3\Omega M)\cdot(\varepsilon h + h^2) + [1+9(\Omega^2 M)h]\cdot\|\Delta p'_k\|. \tag{4.49}$$

Under our assumptions, this inequality holds true for all $\jmath$, such that $2 \le \jmath \le (k-1)$. Hence, we obtain

$$\|\Delta p'_{k+1}\| \le (3\Omega M)\cdot(\varepsilon h+h^2)\cdot\sum_{\jmath=0}^{k-1}[1+9(\Omega^2 M)h]^{\jmath} + [1+9(\Omega^2 M)h]^{k-1}\cdot\|\Delta p'_2\|. \tag{4.50}$$

Noticing that the first term in the right-hand side of (4.50) is proportional to the sum of geometrical progression, we obtain the estimate

$$\begin{aligned}&(3\Omega M)\cdot(\varepsilon h + h^2)\cdot\sum_{\jmath=0}^{k-1}[1+9(\Omega^2 M)h]^{\jmath}\\ &= (3\Omega M)\cdot(\varepsilon h + h^2)\cdot\frac{[1+9(\Omega^2 M)h]^k - 1}{9(\Omega^2 M)h}\\ &\le (\varepsilon + h)[1+9(\Omega^2 M)h]^k.\end{aligned} \tag{4.51}$$

Since $h = 1/(n-1)$ and $k \le (n-2)$, we obtain

$$[1+9(\Omega^2 M)h]^{k-1} < \exp[9\Omega^2 M]. \tag{4.52}$$

The inequalities (4.32), (4.51), and (4.52) imply that

$$\|\Delta p'_{k+1}\| \le \exp[9(\Omega^2 M)](2\varepsilon + h + \varepsilon h + Mh^2). \tag{4.53}$$

Assume that

$$(M+1/2)h^2 < h,\ \forall h \in (0,h_0). \tag{4.54}$$

Since $\varepsilon < 1$ (see (4.37)), it follows from (4.53) that

$$\|\Delta p'_{k+1}\| \le 3\exp[9(\Omega^2 M)](\varepsilon + h). \tag{4.55}$$

Since $\Delta p''_{k+1} = \Delta a_k$, then the inequalities (4.48) and (4.55) imply

$$\begin{aligned}\|\Delta p''_{k+1}\| &\le (3\Omega M)\cdot\varepsilon + 27(\Omega^2 M)\exp[9(\Omega^2 M)](\varepsilon + h)\\ &\le 28(\Omega^2 M)\exp[9(\Omega^2 M)]\cdot(\varepsilon + h).\end{aligned} \tag{4.56}$$

Finally, noticing that $\Delta p_{k+1} = \Delta a_k \cdot h^2/2 + \Delta p'_k \cdot h + \Delta p_k$ and

$$\Delta p_{k+1} = \frac{h^2}{2}\sum_{j=1}^{k}\Delta a_j + h\sum_{j=1}^{k}\Delta p'_j,$$

we obtain from (4.55) and (4.56)

$$\begin{aligned}\|\Delta p_{k+1}\| &\le 28(\Omega^2 M)\exp[9(\Omega^2 M)]\cdot(\varepsilon+h)\cdot(\frac{(n-1)h^2}{2}+(n-1)h)\\ &\le 42(\Omega^2 M)\exp[9(\Omega^2 M)]\cdot(\varepsilon+h). \qquad (4.57)\end{aligned}$$

To prove (4.23) for $j = k$, we notice that

$$\|\tilde{p}_k^{(s)}\| \le \|p_k^{*(s)}\| + \|\Delta p_{k+1}^{(s)}\| \le \frac{M}{2} + \|\Delta p_{k+1}^{(s)}\|. \qquad (4.58)$$

Since $\tilde{p}''_k = \tilde{a}_k(\omega) \in \tilde{G}(M)$, then (4.23) holds true for $\tilde{p''}_k(\xi_k,\omega)$. Assume that the parameters $\varepsilon_0(\Omega, M)$ and $h_0(\Omega, M)$ are chosen sufficiently small, so that in addition to (4.36), (4.37), (4.41), and (4.54), the following inequality holds

$$\frac{M}{2} + 42\Omega^2 M\exp[9\Omega^2 M]\cdot(\varepsilon+h) < \frac{3M}{4},\ \forall(\varepsilon,h)\in(0,\varepsilon_0)\times(0,h_0). \qquad (4.59)$$

Then, it follows from (4.55) and (4.58) that $\tilde{p}'_k(\xi_k,\omega)\in\tilde{G}(M)$, i.e., (4.23) is established for $j = k$.

Show that $F_{k+1}\in\tilde{G}(3M/4)$. It follows from (4.47), (4.55), and (4.59) that

$$\begin{aligned}\|F_{k+1}\| &\le \frac{M}{2} + (2\Omega M)\cdot\varepsilon + 27(\Omega^2 M)\exp[9\Omega^2 M]\cdot(\varepsilon+h)\\ &\le \frac{M}{2} + 28(\Omega^2 M)\exp[9\Omega^2 M]\cdot(\varepsilon+h) < \frac{3}{4}M.\end{aligned}$$

Hence, $F_{k+1}\in\tilde{G}(3M/4)$. Since (4.23) and (4.24) are established, the estimates (4.55)-(4.57) imply (4.25). For the last subinterval $[\xi_{n-2},\xi_{n-1}]$, the proof can be carried out by analogy. However, the Neumann condition at $\xi = 1$ should be taken into account in that case. □

Finally, we show that the estimate (4.25) implies the analogous estimate for the solution $\tilde{\sigma}(\xi)$ of the Inverse Problem II, where

$$\tilde{\sigma}(\xi) = -\frac{1}{L^2\tilde{\omega}_{min}\mu}\cdot\Re[\imath(\tilde{w}'' + \omega(\tilde{w}')^2)], \qquad (4.60)$$

where both functions $\tilde{w}'$ and $\tilde{w}''$ are obtained from the predicted field $\tilde{p}$ and support solution $w_s$ using the formulae (3.53), (3.54).

**Theorem 3.** *Let all conditions of Theorem 2 are satisfied and the following inequality holds*

$$\sup_{\xi\in[0,1]}[\int_{\Omega}^{\infty}|p^{*(s)}(\xi,\tau)|d\tau + |w_s^{(s)}(\xi,\Omega)|] < \alpha; s = 1,2, \qquad (4.61)$$

*where $\alpha > 0$ is sufficiently small constant. Let $\Delta\sigma_i = \tilde{\sigma}(\xi_{i-1}) - \sigma^*(\xi_{i-1})$. Then the following estimate holds*

$$\max_{0\le i\le n}|\Delta\sigma_i| \le \frac{1}{\mu L^2\tilde{\omega}_{min}}K_1(\varepsilon+h+\alpha), \qquad (4.62)$$

*where $K_1 = K_1(\Omega, M) > 0$ is a constant depending only on $\Omega$ and $M$.*

**Proof.** Recall that

$$\tilde{w}'(\xi,\omega) = -\int_\omega^\Omega \tilde{p}'(\xi,\nu)d\nu + \frac{\varphi(\omega)}{\omega} + w_s'(\xi,\Omega), \tag{4.63}$$

$$\tilde{w}''(\xi,\omega) = -\int_\omega^\Omega \tilde{p}''(\xi,\nu)d\nu + w_s''(\xi,\Omega), \tag{4.64}$$

$$w^{*'}(\xi,\omega) = -\int_\omega^\Omega p^{*'}(\xi,\nu)d\nu + \frac{\varphi^*(\omega)}{\omega} - \int_\Omega^\infty p^{*'}(\xi,\nu)d\nu, \tag{4.65}$$

$$w^{*''}(\xi,\omega) = -\int_\omega^\Omega p^{*''}(\xi,\nu)d\nu - \int_\Omega^\infty p^{*''}(\xi,\nu)d\nu. \tag{4.66}$$

By analogy with (4.26), we denote

$$\Delta w_i^{(s)} = \frac{\partial^{(s)}}{\partial\xi^{(s)}}[\tilde{p}_i(\xi_{i-1},1) - p_i^*(\xi_{i-1},1)];\ s = 1,2.$$

Then it follows from (4.60) that

$$\mu L^2\tilde{\omega}_{min}|\Delta\sigma_i| \le |\Delta w_i''| + |\Delta w_i'|\cdot[|\tilde{w}(\xi_{i-1},1)| + |w^*(\xi_{i-1},1)|. \tag{4.67}$$

We estimate all terms in the right-hand side of this inequality. Subtracting (4.66) from (4.64) and taking into account (4.25) and (4.61), we obtain

$$|\Delta w_i''| \le \Omega\cdot K\cdot(\varepsilon + h) + \alpha. \tag{4.68}$$

Similarly, subtracting (4.65) from (4.63) and taking into account (4.19), we obtain

$$|\Delta w_i'| \le \Omega\cdot K\cdot(\varepsilon + h) + \alpha + \frac{\varepsilon}{4}. \tag{4.69}$$

Since $p^* \in G(M/2)$ and $\tilde{p}'(\xi_{i-1},\omega) \in \tilde{G}(M)$, then taking into account (4.19), (4.63), and (4.65), we obtain

$$|\tilde{w}'(\xi_{i-1},1)| + |w^{*'}(\xi_{i-1},1)| \le \Omega M + 2M + \alpha. \tag{4.70}$$

The inequalities (4.67)-(4.70) imply (4.62). □

## 5. Computational experiments

We have performed some computational experiments to demonstrate the feasibility of the proposed algorithm.

### *5.1. Models*

The models used in computational experiments consist of several layers with parallel interfaces (see Figure 1). In all models, the upper layer ($\xi < 0$) contains the air, i.e., a perfect dielectric whose conductivity is assumed to be zero. The inhomogeneous layer ($0 < \xi < 1$) contains the conductive seawater and several sediment layers. The lower layer ($\xi > 1$) contains the homogeneous basement whose conductivity is two order less than the averaged conductivity of the inhomogeneous layer.

In our computational experiments, we use two realistic marine configurations typical for the shallow water Stockholm archipelago, the Baltic sea. Specifically, we adopt the four layer marine configuration

$$\sigma(z) = \begin{cases} 0,\ S \cdot m^{-1} & \text{for } z < 0 \\ 0.70,\ S \cdot m^{-1} & \text{for } 0 \le z < 47\ m \\ 0.14,\ S \cdot m^{-1} & \text{for } 47\ m \le z < 93\ m \\ 0.001,\ S \cdot m^{-1} & \text{for } z \ge 93\ m \end{cases} \tag{5.1}$$

and the five layer marine configuration

$$\sigma(z) = \begin{cases} 0,\ S \cdot m^{-1} & \text{for } z < 0 \\ 0.70,\ S \cdot m^{-1} & \text{for } 0 \le z < 47\ m \\ 0.32,\ S \cdot m^{-1} & \text{for } 47\ m \le z < 55\ m \\ 0.19,\ S \cdot m^{-1} & \text{for } 55\ m \le z < 70\ m \\ 0.001,\ S \cdot m^{-1} & \text{for } z \ge 70\ m. \end{cases} \tag{5.2}$$

Also, we use the realistic parameters in order to construct two more synthetic marine configurations. The third configuration contains a thin highly conductive layer laying on the sediment layer. This thin infinite layer models a mine.

$$\sigma(z) = \begin{cases} 0,\ S \cdot m^{-1} & \text{for } z < 0 \\ 0.70,\ S \cdot m^{-1} & \text{for } 0 \le z < 46\ m \\ 10.0,\ S \cdot m^{-1} & \text{for } 46\ m \le z < 47\ m \\ 0.14,\ S \cdot m^{-1} & \text{for } 47\ m \le z < 93\ m \\ 0.001,\ S \cdot m^{-1} & \text{for } z \ge 93\ m. \end{cases} \tag{5.3}$$

The fourth configuration contains ten layers. It has been constructed to model the sediment conductivity stratification due to porosity.

$$\sigma(z) = \begin{cases} 0,\ S \cdot m^{-1} & \text{for } z < 0 \\ 0.70,\ S \cdot m^{-1} & \text{for } 0 \le z < 47\ m \\ 0.32,\ S \cdot m^{-1} & \text{for } 47\ m \le z < 55\ m \\ 0.19,\ S \cdot m^{-1} & \text{for } 55\ m \le z < 60\ m \\ 0.14,\ S \cdot m^{-1} & \text{for } 60\ m \le z < 70\ m \\ 0.20,\ S \cdot m^{-1} & \text{for } 70\ m \le z < 75\ m \\ 0.40,\ S \cdot m^{-1} & \text{for } 75\ m \le z < 80\ m \\ 0.25,\ S \cdot m^{-1} & \text{for } 80\ m \le z < 87\ m \\ 0.14,\ S \cdot m^{-1} & \text{for } 87\ m \le z < 93\ m \\ 0.001,\ S \cdot m^{-1} & \text{for } z \ge 93\ m. \end{cases} \tag{5.4}$$

It can also be seen that the conductivity of the seawater is $0.7\ S \cdot m^{-1}$ for all four models.

### *5.2. Simulation of sounding data*

To simulate the sounding data $\varphi(\omega)$, we solve numerically the boundary value problem (2.9)-(2.11). Specifically, we reduce this problem to a system of first-order differential equations. This can be accomplished by introducing the new variable

$$y = -\frac{1}{\sqrt{\omega}} \frac{u'}{u}.$$

Then we obtain the Cauchy problem for the linear first-order equation

$$u' + \sqrt{\omega} y u = 0,\ 0 < \xi < 1, \tag{5.5}$$

$$u(0, \omega) = 1 \tag{5.6}$$

and the Cauchy problem for the Riccati equation

$$y' = \sqrt{\omega}(y^2 - i\mathcal{C}^2\sigma(\xi)),\ 0 < \xi < 1, \tag{5.7}$$

$$y(1, \omega) = -\mathcal{C}(i+1)\sqrt{\sigma_b/2}, \tag{5.8}$$

where $\mathcal{C} = L\sqrt{\mu\tilde{\omega}_{min}}$. Setting $y = y_p + z$, where $y_p$ is the particular solution of the Riccati equation, we obtain two Cauchy problems with respect to $y_p$ and $z$

$$y_p' = \sqrt{\omega}(y_p^2 - i\mathcal{C}^2\sigma(\xi)),\ 0 < \xi < 1, \tag{5.9}$$

$$y_p(1, \omega) = -i\mathcal{C}\sqrt{\sigma_b/2} \tag{5.10}$$

and for the Cauchy problem for the Bernoulli equation

$$z' = \sqrt{\omega}(z^2 + 2y_p z),\ 0 < \xi < 1, \tag{5.11}$$

$$z(1, \omega) = -\mathcal{C}\sqrt{\sigma_b/2}. \tag{5.12}$$

Since both the linear (5.5) and Bernoulli (5.11) equations are integrated in the closed form, the sounding data can be represented as

$$\varphi(\omega) = -\sqrt{\omega}[y_p(0, \omega) + t^{-1}(0, \omega)], \tag{5.13}$$

where

$$t(0, \omega) = \sqrt{\omega}\int_0^1 \exp\left(2\sqrt{\omega}\mathcal{I}_1(y_p, \zeta)\right)d\zeta - \mathcal{C}^{-1}\sqrt{2/\sigma_b}\exp\left(2\sqrt{\omega}\mathcal{I}_2(y_p, 0)\right),$$

$$\mathcal{I}_1(y_p, \zeta) = \int_0^\xi y_p(\zeta, \omega)d\zeta,\ \mathcal{I}_2(y_p, \zeta) = \int_\xi^1 y_p(\zeta, \omega)d\zeta,$$

It can be seen from (5.13) that the function $\varphi(\omega)$ is actually determined by the particular solution $y_p$ of the Riccati equation. We solve numerically the problem (5.9)-(5.10) using the fourth-order Runge-Kutta method. Because of algorithmic and roundoff errors, the simulated data are always slightly perturbed. The relative level of the total error has been estimated by testing the Riccati solver against the analytical solutions of the forward problem for the three and four layer configurations. Based on the test results, we are confident that it does not exceed $5 \cdot 10^{-5}$. Figure 2 shows the comparison between the analytical and numerical solutions in terms of the logarithmic apparent resistivity $\rho_a = \log_{10}[\omega\mu/|\varphi(\omega)|^2]$, which is usually used in practice to represent the data. For the sake of vizualisation, here and below we display the dimensional frequency $\tilde{f} = \tilde{\omega}/2\pi$. Although such slightly perturbed data are used in all computational experiments, in this paper we do not model the noisy data. Instead, we focus on simulating the incomplete data and extending them to more broad frequency band.

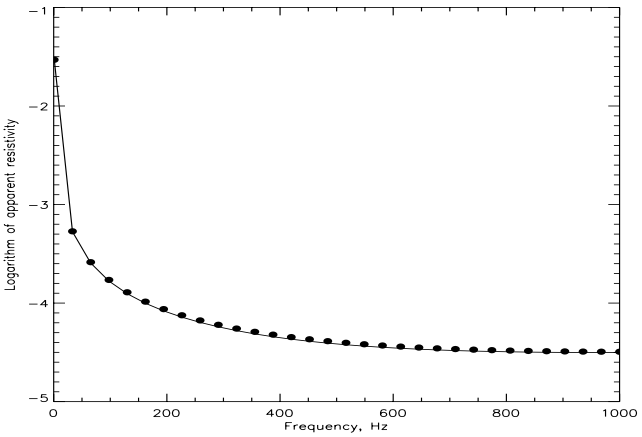


**Figure 2.** The apparent resistivity for the four layer medium. The analytical solution (solid) in comparison with the numerical solution (filled bullets) for the frequency band [1, 1000]Hz.

*5.3. Implementation of the sequential minimisation procedure*

Following the procedure of sequential minimisation (see Section 3.3.3), we first discretize the interval $[1, \Omega]$ by using a semi-uniform grid because of the strong filtering effect of the seawater. Specifically, we use a uniform grid with sufficiently small step when discretizing the interval $[1, 50]$ and another uniform grid with much larger step when discretizing its complement. As a result, the discrete analogues of complex valued functions $w, w', w'', p, p', p'', a_\imath, F, \Psi, \hat{k}_b$ defined on the interval $[1, \Omega]$ for each fixed $\xi$ generate the complex vectors belonging to $C^m$. For convenience, we shall preserve the same notations for the corresponding vectors, so that the symbol $\omega$ denotes below a real vector belonging to the Eucleaden space $R^m$. Also, we precompute the vectors $\hat{F}$ and $\hat{\Psi}$

$$\hat{F} = \frac{\hat{\varphi}}{\omega}[\frac{\hat{\varphi}}{\omega} - 2\hat{\varphi}'],$$
$$\hat{\Psi} = \frac{1}{\omega}[\frac{\hat{k}_b(\omega) + \hat{\varphi}(\omega)}{\omega} - \hat{k'}_b(\omega) - \hat{\varphi}'(\omega)].$$

Here, the symbol $'$ means a certain finite-difference approximation of the first derivative of the function $\varphi(\omega)$. To compute $\hat{\varphi}'$, we use Stechkin's regularisator (see, e.g., [24]).

To solve numerically all $n-1$ minimisation problems (3.46) indicated in Section 3.3.3, the set $\tilde{G}(M)$ needs to be specified. In general, the construction of constraints can be accomplished in several ways. If no *a priori* information about the problem to be solved is available, we take the following nonlinear constraints for each fixed $\imath = 1, 2, ..., n-1$

$$0 \le |a_\imath(\omega)| \le B,$$

where $a_\imath = (\Re(a_\imath), \Im(a_\imath))$ is the $2m$-dimensional real vector and $B > 0$ is a certain constant. As a result of finite-dimensional approximation, we obtain $n-1$ sets $\mathcal{P}_\imath$ of

constraints. The next stage consists of solving the minimisation problems

$$argmin\{J_{\lambda,\imath}(a_\imath) : |a_\imath| \in \mathcal{P}_\imath\}, \tag{5.14}$$

In the mathematics literature (see, e.g., [15]), there are available several numerical methods for solving the constrained minimisation problems. In our computational experiments, we use the Generalised Reduced Gradient Method (GRGM) (see, e.g., [25]) because of the nonlinear objective function and constraints. We outline briefly the descent scheme of sequential minimisation in the algorithmic form

$a_{start} = \hat{F}$
**FOR i=1, n-1 DO BEGIN**
*Compute* $a_{3\imath}$
**FOR k=1, 2, ... DO BEGIN**
$a_\imath^{(k+1)} = a_\imath^{(k)} - \beta_k s_k$
**IF** $|\Delta_k J_{\lambda\imath}| \leq$ **STOP THEN GOTO JUMP**
**ENDFOR**
**JUMP:**
$\tilde{a}_\imath = a_\imath^{(k_{stop})}$
*Compute* $\tilde{\rho}(\tilde{a}_\imath),\ \tilde{\eta}_\imath(\tilde{a}_\imath)$
$a_{start} = \tilde{a}_\imath$
**ENDFOR**,

where $-s_k$ is the direction of descent. The parameters $\beta_k$ are chosen, so that the relaxation condition, i.e., $J_{\lambda,\imath}(a_\imath^{(k+1)}) < J_{\lambda,\imath}(a_\imath^{(k)})$, is fulfilled. We accept the $k$th iterate $a_\imath^k$ as an approximate minimiser if either the variation $|\Delta_k J_{\lambda,\imath}|$ between two consecutive iterations of the objective function is less than **STOP** or the Kuhn-Tucker optimality conditions are approximately satisfied to **STOP**. In computational experiments, the number **STOP** is set up $10^{-5}$. It should also be pointed out that being a descent method, the GRGM requires the starting vectors to be specified for each subinterval $(\xi_{i-1}, \xi_i], (\imath = 1, ..., n-1)$. The following procedure is adopted for choosing the starting vectors. It follows from (3.30)-(3.32) and (4.5) that the vector $\hat{F}_1$ depending on the data $\hat{\varphi}$ can be taken as a starting vector $a_1^{start}$. Then, we take consecutively $a_\imath^{start} = \tilde{a}_{\imath-1}, (\imath = 2, ..., n-1)$. In the sequential minimisation algorithm, the starting vectors are determined either from the data $\hat{\varphi}(\omega)$ or from the preceding approximate minimisers $\tilde{a}_\imath,\ (\imath = 1, ..., n-1)$. Thus, we eliminate the uncertainty in choosing a starting vector inherent in the Newton-like methods.

The procedure results in the finite set of $m$-dimensional complex valued vectors $\{\tilde{a}_\imath\}_{\imath=1}^{n-1}$. Given this set, the first derivative of the predicted field $p(\xi, \omega)$ if computed from Eq. (3.51). Then, the approximate conductivity profile $\tilde{\sigma}(\xi)$ is directly computed from Eqs. (3.55)-(3.58). In computational experiments, all integrals are computed using Gaussian quadrature formulas.

*5.4. Numerical results*

We apply the sequential minimisation algorithm to the simulated data indicated in Section 5.2. In computational experiments, we use the CWFs (see Eq. (3.24)) with sufficiently large parameter $\lambda$ varying from 200 to 500. For such values of $\lambda$, the changes in the reconstructed conductivity distribution are small. The CWFs provide sufficiently high values of the convexity parameter $\rho$ and, hence, sufficiently high rate of convergence of the GRGM. For the four, five, and ten layer models, the interval $[0, L]$ is discretised into $n - 1 = 31$ subinterval, whereas it is discretised into $n - 1 = 127$ subintervals for two other models.

*5.4.1. Inversion of incomplete data* It has been mentioned in Section 3.2 that the "cutting" frequency $\Omega$ does not necessarily coincide with the upper bound $\omega_{max}$ of the frequency band. Due to technological or logistic reasons, the upper bound $\omega_{max}$ often is much less than the frequency $\Omega$ providing sufficient accuracy of the approximate model (3.18)-(3.20). Therefore, we first simulate the incomplete data in the frequency band $[1, 200]$ Hz and apply the sequential minimisation algorithm for these incomplete data. Figure 3 shows the result of inversion (asterisks) for $B = 10^{-2}$. We observe

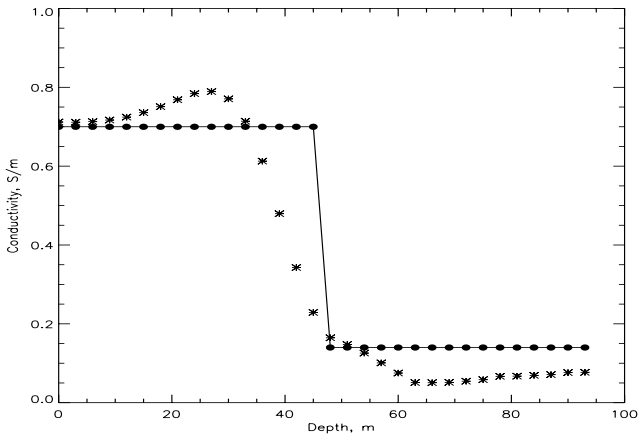


**Figure 3.** Comparison the "exact" solution (solid) for the four layer configuration with the conductivity profiles recovered from the incomplete (asterisks) and extended (filled bullets) data.

that if no *a priori* information is available, the recovered conductivity profile differs significantly from the "exact" profile. This is due to incomplete data and relatively large approximation error. Under such conditions, the high resolution of the so-called fine structure of $\sigma(z)$ cannot be expected for any regularising algorithm including the proposed one. However, it is well-known from the theory of ill-posed problems (see, e.g., [14]) that using *a priori* information about the specific problem to be solved may improve the accuracy of a regularised solution. Therefore, we focus further on exploiting such an information in the sequential minimisation algorithm.

*5.4.2. Using a priori information* To improve the accuracy of reconstruction, we use *a priori* information about the problem. Specifically, we employ the concept of a support solution. This concept consists of the following. Since the highly conductive seawater plays the role of a low pass filter with respect to EM field propagated through the water column, the gradients of $\varphi(\omega)$ corresponding to many realistic distributions of conductivity differ slightly at sufficiently high frequencies, say at frequencies greater than $\omega_{max}$. Moreover, the conductivity of the seawater $\sigma_w$ can be estimated from the direct measurements. Therefore, one can introduce the three layer support model

$$\sigma(z) = \begin{cases} 0 & \text{for } z < 0 \\ \sigma_w & \text{for } 0 \le z < L \\ \sigma_b & \text{for } z \ge L \end{cases} \tag{5.15}$$

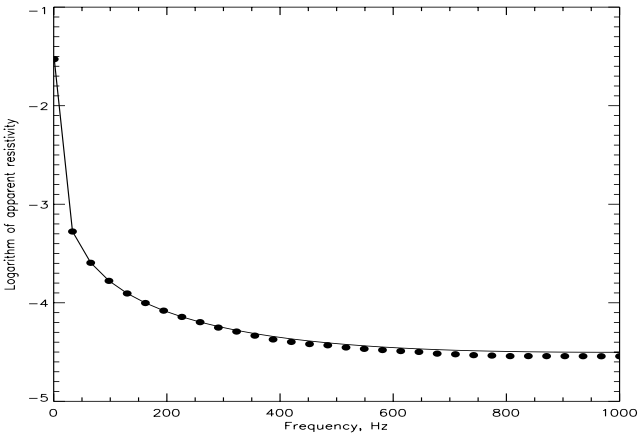


**Figure 4.** The "exact" data (solid) for the four layer model in comparison with the extended data (5.16) for the frequency band [200, 1000] Hz (filled bullets).

It should be emphasised that the proximity of this model to the models (5.1) - (5.4) is not required when exploiting the sequential minimisation algorithm. We can then find the analytical solution of the forward problem (2.9)-(2.11) for the support model and use it for extending the sounding data $\varphi(\omega),\ \omega \in [1, \omega_{max}]$ on the interval $(\omega_{max}, \Omega]$. Also, this allows us to decrease significantly the approximation error. As an example, we describe below a simple heuristic procedure for such an extension.

Let $\varphi_3(\omega)$ be the data obtained from this solution. From *a priori* information, the gradients of both functions $\varphi(\omega)$ and $\varphi_3(\omega)$ are sufficiently close in the interval $\omega \in (\omega_{max}, \Omega]$. This means that one can extend the data $\varphi(\omega)$ on the interval $(\omega_{max}, \Omega]$ by adding $\varphi_3(\omega),\ \omega \in (\omega_{max}, \Omega]$ and eliminating the jump at $\omega = \omega_{max}$. Specifically, the extended data are defined as

$$\hat{\varphi}(\omega) = \begin{cases} \varphi(\omega) & [1, \omega_{max}] \\ \hat{\varphi}_3(\omega) & (\omega_{max}, \Omega], \end{cases} \tag{5.16}$$

where

$$\hat{\varphi}_3(\omega) = \begin{cases} \varphi_3(\omega) + \Delta(\omega_{max}) & \text{if } \varphi(\omega_{max}) \ge \varphi_3(\omega_{max}) \\ \varphi_3(\omega) - \Delta(\omega_{max}) & \text{if } \varphi(\omega_{max}) < \varphi_3(\omega_{max}), \end{cases} \tag{5.17}$$

and $\Delta(\omega_{max}) = \varphi(\omega_{max}) - \varphi_3(\omega_{max})$. Figure 4 shows the result of extending the data on the interval (200, 1000] Hz in terms of the logarithmic apparent resistivity for the four layer model. After extending the data, the level of the total relative error does not exceed $10^{-4}$ for all four models indicated above.

Given the three layer support configuration, we compute consecutively the vectors $u_3,\ p_3,\ a_{3\imath}$ and derive $m$ nonlinear constraints for each fixed $\imath = 1, 2, ..., n-1$ for minimisation problems (5.14). These constraints are as follows

$$0 \le |a_\imath(\omega)| \le \alpha |a_{3\imath}(\omega)|,$$

where $\alpha > 1$ is a certain number. We have found that the minimisers of corresponding minimisation problems were not significantly changed if $\alpha \in [2, 100]$. In Figure 5, we plot these constraints for the first subinterval, i.e., $\imath = 1$ for the four layer model.

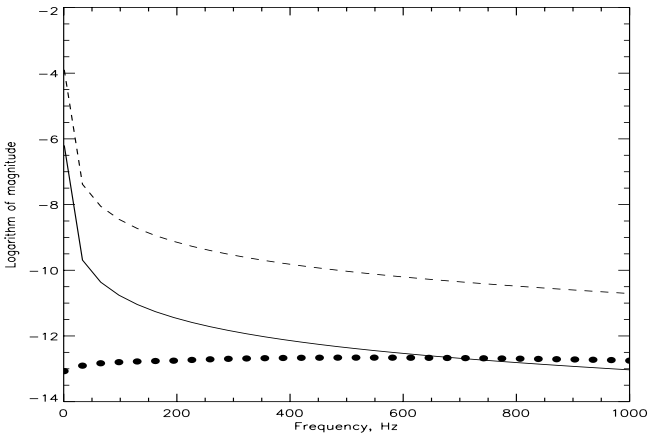


**Figure 5.** The magnitude of the "exact" coefficient $a_1$ (solid), constraint (dashed) and starting vector (filled bullets).

The incomplete data simulated in the frequency band $[1, 200]$ Hz have been extended to the band $(200, 1000]$ Hz using the corresponding three layer support configurations. Also, we use the constraints derived from the support model. Figures 3 (bullets) and 6 demonstrate the performance of the sequential minimisation algorithm for the realistic shallow water sediment configurations. In Figure 3, we see that the accuracy of the recovered conductivity profile can be significantly improved when using *a priori* information in the form indicated above. In Figure 7, we plot the reconstructed profile for the synthetic ten layer sediment configuration in order to demonstrate the resolution power of the sequential minimisation algorithm when using *a priori* information. Finally, Figure 8 shows its performance when identifying the mine modelled as an infinite highly conductive layer.

Thus, we have demonstrated that in the case of "noiseless" data, using *a priori* information is crucial for providing the high accuracy of reconstruction. It should also be pointed out that the similar situation takes place when applying the Newton-like methods to 1-D MT(EM) frequency sounding "noiseless" data and using *a priori*

information about the interface positions. As an example, we refer to the paper [26], in which the performance of the Marquardt-Levenberg and regularised Newton-Kantorovich methods was numerically studied for the same marine configurations. The results of reconstruction were similar to the results indicated in Figures 3 (filled bullets) and 6 only if the "good" starting vectors were chosen.

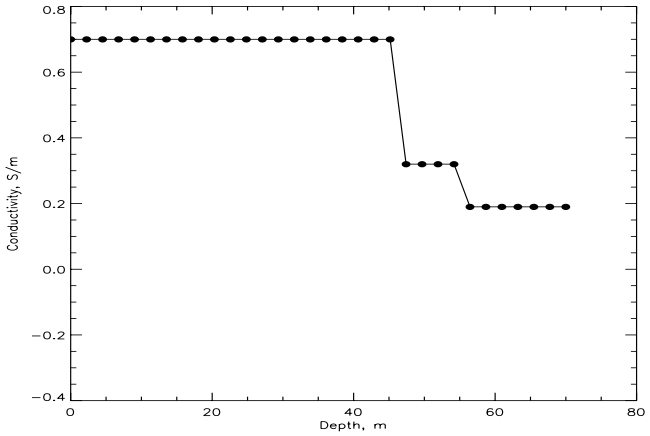


**Figure 6.** The reconstructed conductivity profile (filled bullets) in comparison with the "exact" solution (solid) for the five layer configuration.

## 6. Conclusions

We have constructed the sequential minimisation algorithm that implements the convexification approach to 1-D inverse problems of electromagnetic frequency sounding. It can also be applied to solve the inverse problems for more general equation $u'' + [\omega^2\alpha(\xi) + \imath\omega\beta(\xi) + \gamma(\xi)]u = 0$. Whereas the gradient or Newton-like methods require *a priori* information about the "good" starting vector, the proposed algorithm utilises the sounding data providing the convergence to the approximate solution on the correctness set. The procedure of sequential minimisation can be given the clear physical interpretation. Indeed, transforming the original inverse problem to an auxiliary one, we reformulate it in terms of prediction of the electromagnetic field from the surface into an inhomogeneous layer. Since the field prediction problem is, in general, unstable, we construct the layer stripping-like procedure dividing the spatial domain of the unknown conductivity distribution into a finite set of subintervals and approximating in each subinterval the spatial dependence of the field by a quadratic polynomial with frequency dependent coefficients. Using the Carleman weight functions, we stabilise the field prediction when advancing into the inhomogeneous layer. Once the predicted field is computed, the inversion of sounding data is explicitly performed.

Also, we indicate here several prospective directions for research. First, to make the sequential minimisation algorithm applicable to the real data, we need to test its performance for noisy data and improve the algorithm if required. Second, it is our

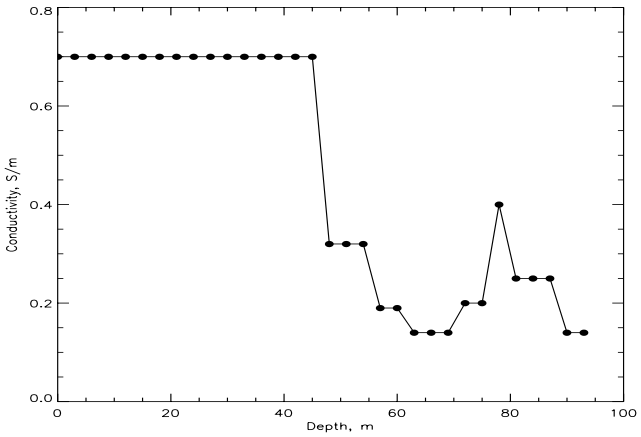


**Figure 7.** The reconstructed conductivity profile (filled bullets) in comparison with the "exact" solution (solid) for the ten layer configuration.

intention to construct some iterative algorithms exploiting the contraction property indicated in Lemma 5. Third, we plan to extend our approach to some inverse problems of acoustic frequency sounding of absorbing media and infrared optical sensing of a human body. We also plan to extend the sequential minimisation algorithm to the 2-D and 3-D models.

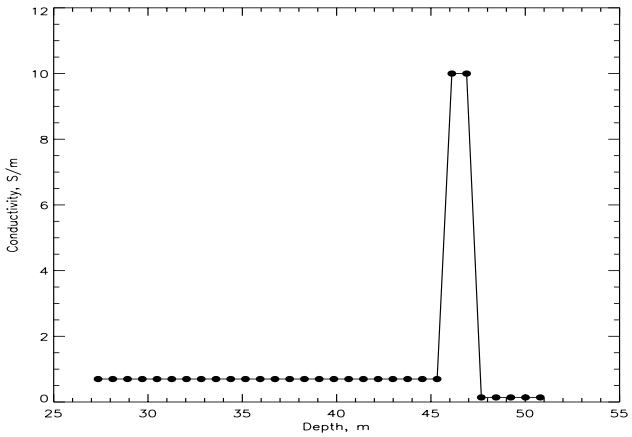


**Figure 8.** The reconstructed conductivity profile (filled bullets) in comparison with the "exact" solution (solid) for the five layer configuration containing the modelled mine layer.

## Acknowledgments

We thank Dr Krylstedt and Dr Mattsson for supplying one of authors (AT) with particular marine configurations of the Stockholm archipelago used in computational experiments. We also thank one of anonymous referees whose friendly and constructive comments have helped to improve the paper.

## Appendix A

In this appendix, we outline briefly the derivation of two models of electromagnetic frequency sounding exploiting the vertical magnetic (VMD) and horizontal electric (HED) dipoles. Our goal is to demonstrate that both the magnetotelluric and electromagnetic model problems are similar.

Assume that the VMD is placed at the surface $z = 0$, and the frequency dependence of the vertical component of the magnetic field $H_z$ is measured. Introducing the cylindrical coordinates $(r, \theta, z)$, taking into account the axial symmetry and expressing the components of electromagnetic field via the scalar potential $U$, we obtain from Maxwell's equation that $H_z = IS[U''(r, z, \tilde{\omega}) - k^2(z, \tilde{\omega})U(r, z, \tilde{\omega})]$, where $I$ is the electric current and $S$ is the area of the loop. Assuming that the scalar potential is representable via its Hankel (Fourier-Bessel) transform, i.e.,

$$U(r, z, \tilde{\omega}) = (4\pi)^{-1} \int_0^\infty J_0(\nu r) u(z, \nu, \tilde{\omega}) \nu d\nu$$

and taking into account the continuity conditions at both interfaces $z = 0$ and $z = L$, we arrive to the governing model

$$u''(z, \nu, \tilde{\omega}) - (\nu^2 + k^2(z, \tilde{\omega}))u(z, \nu, \tilde{\omega}) = 0, \ 0 < z < L, \tag{6.1}$$

$$u'(0, \nu, \tilde{\omega}) + \nu u(0, \nu, \tilde{\omega}) = -2\delta(z), \tag{6.2}$$

$$u'(L, \nu, \tilde{\omega}) + \sqrt{\nu^2 + k_b(\tilde{\omega})}u(L, \nu, \tilde{\omega}) = 0, \tag{6.3}$$

In the case of the HED oriented, say, along the $x$ axis, the electromagnetic field can be expressed via the vector potential $\mathbf{A} = (A_x, 0, A_z)$ whose components satisfy the equations

$$\nabla^2 A_x - k^2 A_x = -Il\delta(\mathbf{r}),$$

$$\nabla \cdot (\sigma^{-1}(z)\nabla A_z) - i\tilde{\omega}\mu A_z = \frac{\partial A_x}{\partial x}(\sigma^{-1}(z))'$$

and continuity conditions at interfaces. Here, $Il$ is the current moment, Again, representing both components of the vector potential via their Hankel transforms

$$A_x(r, z, \tilde{\omega}) = \frac{Il}{4\pi} \int_0^\infty J_0(\nu r) u(z, \nu, \tilde{\omega}) \nu d\nu,$$

$$A_z(r, z, \tilde{\omega}) = \frac{Il}{4\pi} \frac{\partial}{\partial x} \int_0^\infty J_0(\nu r)[v(z, \nu, \tilde{\omega}) - \nu^{-1} u'(z, \nu, \tilde{\omega})] d\nu,$$

we obtain two models, i.e.,

$$u''(z, \nu, \tilde{\omega}) - (\nu^2 + k^2(z, \tilde{\omega}))u(z, \nu, \tilde{\omega}) = 0, \ 0 < z < L, \tag{6.4}$$

$$u'(0, \nu, \tilde{\omega}) - \nu u(0, \nu, \tilde{\omega}) = -2\delta(z), \tag{6.5}$$

$$u'(L, \nu, \tilde{\omega}) + \sqrt{\nu^2 - k_b(\tilde{\omega})}u(L, \nu, \tilde{\omega}) = 0, \tag{6.6}$$

and

$$(v'\sigma^{-1}(z))' - (\nu^2 + k^2(z, \tilde{\omega}))\sigma^{-1}(z)v(z, \nu, \tilde{\omega}) = 0, \ 0 < z < L, \tag{6.7}$$

$$v(0, \nu, \tilde{\omega}) = 2\nu^{-1}, \tag{6.8}$$

$$v'(L, \nu, \tilde{\omega}) + \frac{\sigma(L)}{\sigma_b}\sqrt{\nu^2 - k_b(\tilde{\omega})}v(L, \nu, \tilde{\omega}) = 0, \tag{6.9}$$

As expected, the MT model (2.6)-(2.8) and the EM models (6.1)-(6.3) and (6.4)-(6.6) are sufficiently close if $\nu = 0$.

## Appendix B

**Proof of Lemma 1.** Since (2.6)-(2.8) is the Sturm-Liouville problem, it is sufficient to prove its uniqueness. Assume that this problem has two different solutions $u_1$ and $u_2$ and $v = u_1 - u_2$. It satisfies the boundary value problem

$$v''(z,\tilde{\omega}) - i\mu\tilde{\omega}\sigma(z)v(z,\tilde{\omega}) = 0,\ 0 < z < L, \tag{6.10}$$

$$v(0,\tilde{\omega}) = 0, \tag{6.11}$$

$$v'(L,\tilde{\omega}) + k_b(\tilde{\omega})v(L,\tilde{\omega}) = 0, \tag{6.12}$$

Let $\overline{v}$ be the complex conjugate of the function $v$. Multiplying (6.10) by $\overline{v}$ and integrating from 0 to $L$ over $z$, we obtain

$$\int_0^L |v'|^2 dz + i\mu\tilde{\omega}\int_0^L \sigma(z)|v|^2 dz + k_b|v(L,\tilde{\omega})|^2 = 0.$$

Separating the real and imaginary parts, we obtain

$$\int_0^L |v'|^2 dz + \frac{1}{\sqrt{2}}\sqrt{\mu\tilde{\omega}\sigma_b}|v(L,\tilde{\omega})|^2 = 0,$$

$$\mu\tilde{\omega}\int_0^L \sigma(z)|v'|^2 dz + \frac{1}{\sqrt{2}}\sqrt{\mu\tilde{\omega}\sigma_b}|v(L,\tilde{\omega})|^2 = 0.$$

Hence, $v(z,\tilde{\omega}) \equiv 0$.

Show that $u(z,\tilde{\omega}) \neq 0$ on $[0,L]\times[\tilde{\omega}_{min},\infty)$. Assume that the opposite is true, i.e., there exists a pair $(z_0,\tilde{\omega}_0)$, such that $u(z_0,\tilde{\omega}_0) = 0,\ (z_0,\tilde{\omega}_0) \in [0,L]\times[\tilde{\omega}_{min},\infty)$. Because of (2.7), $z_0 \neq 0$. Suppose $z_0 \in (0,L)$. It follows from Lemma 1 that $u(z,\tilde{\omega}_0) = 0$ for $z \in [z_0,L]$. This implies that $u(z,\tilde{\omega}_0) = 0$ for all $z \in [0,L]$, which contradicts to (2.7). Let $z_0 = L$. It follows from (2.8) that $u'(z_0,\tilde{\omega}_0) = u(z_0,\tilde{\omega}_0) = 0$. But this leads to $u(z,\tilde{\omega}_0) = 0$ for all $z \in [0,L]$. □

## Appendix C

In this appendix, we dicsuss the uniqueness results for the Inverse Problem I and II. We first point out that the solution $u(z,\tilde{\omega})$ of the boundary value problem (2.6)-(2.8) is an analytical function of the real variable $\tilde{\omega}$. Hence, the uniqueness result for the Inverse Problem II can easily be obtained from the uniqueness result for the Inverse Problem I via analytic continuation with respect to $\tilde{\omega}$. Therefore, we consider below the Inverse Problem I only. In the case of piecewise analytic function $\sigma(z)$, the uniqueness theorem for this problem was first proven in [3]. If $\sigma(z) \in C^2[0,\infty),\ \sigma(z) > const > 0,\ \sigma_b > 0$, the analogous result can also be established. We outline briefly the proof.

First, we observe that the solution of the problem (2.6)-(2.8) can be extended on the half-axis $(0,\infty)$ via solving the problem

$$u''(z,\tilde{\omega}) - i\mu\tilde{\omega}\sigma(z)u(z,\tilde{\omega}) = 0,\ 0 < z < \infty, \tag{6.13}$$

$$u(0,\tilde{\omega}) = 1, \tag{6.14}$$

$$\lim_{z\to\infty}[u'(z,\tilde{\omega}) + k_b(\tilde{\omega})u(z,\omega)] = 0. \tag{6.15}$$

It can be proven that the solutions of the boundary value problem (2.6)-(2.8) and (6.13)-(6.15) coincide for $z \in [0, L)$. Consider an auxiliary hyperbolic boundary value problem

$$\mu\sigma(z)v_{tt} = v_{zz},\ 0 < z < \infty, \tag{6.16}$$

$$v(0,t) = \delta(t), \tag{6.17}$$

$$v(z,0) = v_t(z,0) = 0. \tag{6.18}$$

We formulate the following problem.

**Inverse Problem III.** *Given the function*

$$\psi(t) = v_z(0,t),\ 0 < t < \infty. \tag{6.19}$$

*Find the function $\sigma(z)$, for which the equations (6.16)-(6.19) are satisfied.*

The following formula holds for sufficiently large positive $\tilde{\omega}$

$$u(z,\tilde{\omega}) = \int_0^\infty \exp\left(-\sqrt{i\tilde{\omega}}t\right)v(z,t)dt. \tag{6.20}$$

Since (6.20) is a Laplace-like transform, it is the one-to-one operator. Thus, the uniqueness result for the Inverse Problem I follows from the uniqueness result for the Inverse Problem III.

Consider the new variable $x = x(z)$ [20]

$$x = \int_0^z \sqrt{\mu\sigma(y)}dy \tag{6.21}$$

and introduce the function

$$S(x) = \sqrt{\frac{\sigma(0)}{\sigma(z(x))}}. \tag{6.22}$$

Let

$$a(x) = \frac{S''(x)}{S(x)} - 2[\frac{S'(x)}{S(x)}]^2. \tag{6.23}$$

Then the boundary value problem (6.16)-(6.18) can be reduced to the problem

$$v_{tt} = v_{xx} + a(x)v,\ 0 < x < \infty, \tag{6.24}$$

$$v(0,t) = \delta(t), \tag{6.25}$$

$$v(x,0) = v_t(x,0) = 0, \tag{6.26}$$

and the data for this problem are

$$v_x(0,t) = \frac{1}{\sqrt{\mu\sigma(0)}}\psi(t). \tag{6.27}$$

For brevity, we assume that both values $\sigma(0)$ and $\sigma'(0)$ are known. Then, if the function $a(z)$ is known, then the fucntion $\sigma(z)$ is determined. The uniqueness result for a certain hyperbolic inverse problem, which is similar to the problem (6.24)-(6.26), was proven in [20], [27] via obtaining the system of the Volterra-like integral equations of the second kind. The proof of the uniqueness result for the problem (6.24)-(6.26) can be analogously obtained. Thus, the following theorem is true.

**Theorem 4.** *Both the Inverse Problem I and II have at most one solution $\sigma(z)$ satisfying the following conditions: (1) $\sigma(z) \in C^2[0,\infty)$, (2) $\sigma(z) \geq const > 0$, (3) $\sigma(z) = \sigma_b = const$ for $z > L$, and (4) the values $\sigma(0)$ and $\sigma'(0)$ are known.*

In addition, it follows from (6.20)-(6.26) that the asymptotic behavior of the functions $\partial^s u/\partial z^s(z,\tilde{\omega})$ is

$$\frac{\partial^s}{\partial z^s}\exp\left[-\sqrt{i\tilde{\omega}\mu}\cdot\int_0^z\sqrt{\sigma(y)}dy\right]\cdot[1+O(\tilde{\omega}^{-1/2})],\ \tilde{\omega}\to\infty,\ s=0,1,2.$$

This justifies the convergence of integrals in (3.6), (4.65), and (4.66). In dimensionless variables, the asymptotic formula has the form

$$\sqrt{2\pi}\frac{\partial^s}{\partial\xi^s}\exp\left[-\sqrt{i\omega\mu}\cdot\int_0^{L\xi}\sqrt{\sigma(\zeta)}d\zeta\right]\cdot[1+O(\omega^{-1/2})],\ \omega\to\infty,\ s=0,1,2.$$

## References


[1] Klibanov M V and Timonov A 2001 A new slant on the inverse problems of electromagnetic frequency sounding: 'convexification' of a multiextremal objective function via the Carleman weight functions *Inverse Problems* **17** 1865-87

[2] Tikhonov A N 1950 On determining the electrical characteristics of deep layers of the earth crust *Sov.Math.Dokl.* **2** 295-97

[3] Tikhonov A N 1965 Mathematical basis of the theory of electromagnetic soundings *U.S.S.R. Comput.Math.Mathemat.Phys.* **5** 207-11

[4] Cagniard L 1953 Basic theory of the magnetotelluric method of geophysical prospecting *Geophysics* **37** 605-35

[5] Berdichevsky M N and Zhdanov M S 1984 *Advanced Theory of Deep Geomagnetic Sounding* (Elsevier Science Publishing Inc.)

[6] Constable S C 1990 Marine electromagnetic induction studies *Surv.Geophys.* **11** 303-27

[7] Palshin N A 1996 Oceanic electromagnetic studies: A review *Surv.Geophys.* **17** 455-91

[8] *Proc. MARELEC (London, UK, June 1997; Brest, France, July 1999; Stockholm, Sweden, July 2001)*

[9] Haber E, Asher U M, and Oldenburg D 2000 On optimization techniques for solving nonlinear inverse problems *Inverse Problems* **16** 1263-80

[10] Newman G A and Harvesten G M 2000 Solution strategies for two- and three-dimensional electromagnetic inverse problems *Inverse Problems* **16** 1357-75

[11] Dmitriev V I and Alekseeva N V 1984 An algorithm for the numerical solution of the inverse problem of MT sounding *Software Library for Geophysics* (Moscow State University, Moscow)(in Russian)

[12] Alexander J C and Yorke J A 1978 The homotopy continuation method: numerically implementable topological procedures *Trans.Am.Math.Soc.* **242** 271-84

[13] Ramlau R 2002 A steepest descent algorithm for the global minimization of the Tikhonov functional *Inverse Problems* **18** 381-403

[14] Bakushinsky A B and Goncharsky A V 1994 *Ill-Posed Problems: Theory and Applications* (Kluwer Academic Publishers, Dodrecht)

[15] Himmelblau D M 1972 *Applied Nonlinear Programming* (McGraw-Hill)
[16] Curtis E B and Morrow J A 1990 Determining the resistors in a network *SIAM J.Appl.Math.* **50** 931-41
[17] Somersalo E, Cheney M, Isaacson D and Isaacson E L 1991 Layer-stripping: a direct numerical method for impedance imaging *Inverse Problems* **7** 899-926
[18] Chen Y, Rokhlin V 1992 On the inverse scattering problem for the Helmholtz equation in one dimension *Inverse Problems* **8** 365-91
[19] Silvester J and Winebrenner D 1998 Linear and nonlinear inverse scattering *SIAM J.Appl.Math.* **59** 669-99
[20] Isakov V 1998 *Inverse Problems for Partial Differential Equations* (Springer, New York)
[21] Klibanov M V 1997 Global convexity in a three-dimensional inverse acoustic problem *SIAM J.Math.Anal.* **28** 1371-88
[22] Tikhonov A N 1943 On stability of inverse problems *Sov.Math.Dokl.* **39** 195-98
[23] Lavrentiev M M, Romanov V G, and Shishatskii S P 1986 *Ill-Posed Problems of Mathematical Physics and Analysis* (AMS, Providence R.I.)
[24] Arestov V V 1996 Approximation of unbounded operators by bounded operators and related extremal problems *Russian Math.Surv.* **51** 1093-1126
[25] Ladon L S, Waren A D, Jain A, and Ratner M 1978 Design and testing of a Generalised Reduced Gradient Code for nonlinear programming ACM Transactions on Mathematical Software **4** 34-50
[26] Krylstedt P, Mattsson J, and Timonov A 2001 Numerical modelling of electromagnetic frequency sounding in marine environments: A comparison of local optimization techniques *Proc. MARELEC (Stockholm, Sweden, July 2001).*
[27] Romanov V G 1987 *Inverse Problems of Mathematical Physics* (VNU, Utrecht)